AD-A070 806 DREYFUS-PELLMAN CORP STAMFORD CT F/G 1/3
NON-CONTACTING ELECTRO-OPTICAL CONTOURING OF HELICOPTER ROTOR B--ETC(U)
DEC 78 M G DREYFUS, A PELLMAN DAAK50-78-C-0008
UNCLASSIFIED USAAVRADCOM-TR-79-30 NL

| OF |
AD
A070806

END
DATE
FILMED
8-79
DDC

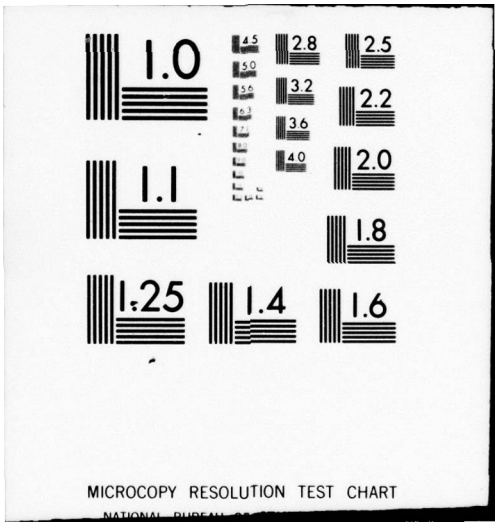
1.0
1.1
1.25
1.4
1.6
1.8
2.0
2.2
2.5
2.8
3.2
3.6
4.0
4.5
5.0
MICROCOPY RESOLUTION TEST CHART

LEVEL II

REPORT: CONTRACT DAAK-50-78-C-0008 (P6D)

NON-CONTACTING ELECTRO-OPTICAL CONTOURING OF HELICOPTER ROTOR BLADES

APPROVED FOR PUBLIC RELEASE;
DISTRIBUTION UNLIMITED

Marc G. Dreyfus
Arnold Pellman
Dreyfus-Pellman Corporation
93 Prospect Street
Stamford, Connecticut 06901

11 December 1978
Final Technical Report

Prepared For:

U. S. Army Aviation Research & Development Command
P. O. Box 209
DRDAV-PDE
St. Louis, Missouri 63166

The findings in this report are not to be construed as an official Department of the Army position unless so designated by other authorized documents.

SECURITY CLASSIFICATION OF THIS PAGE (When Data Entered)

REPORT DOCUMENTATION PAGE

READ INSTRUCTIONS BEFORE COMPLETING FORM

1. REPORT NUMBER: USAAVRADCOM TR-79-30
2. GOVT ACCESSION NO.
3. RECIPIENT'S CATALOG NUMBER

4. TITLE (and Subtitle): NON-CONTACTING ELECTRO-OPTICAL CONTOURING OF HELICOPTER ROTOR BLADES
5. TYPE OF REPORT & PERIOD COVERED: Final - October 1977-October 1978
6. PERFORMING ORG. REPORT NUMBER

7. AUTHOR(s): Marc G. Dreyfus, Arnold Pellman
8. CONTRACT OR GRANT NUMBER(s): DAAK50-78-C-0008 (P6D)

9. PERFORMING ORGANIZATION NAME AND ADDRESS: Dreyfus-Pellman Corporation, 93 Prospect St., Stamford, Ct. 06901
10. PROGRAM ELEMENT, PROJECT, TASK AREA & WORK UNIT NUMBERS: AMS CODE: 53970M 6350, M766350

11. CONTROLLING OFFICE NAME AND ADDRESS: U.S. Army Aviation Res. & Dev. Cmd. DRDAV-PDE, St. Louis, MO. 63166
12. REPORT DATE: 11 Dec [redacted]78
13. NUMBER OF PAGES

14. MONITORING AGENCY NAME & ADDRESS(if different from Controlling Office)
15. SECURITY CLASS. (of this report): Unclassified
15a. DECLASSIFICATION/DOWNGRADING SCHEDULE

16. DISTRIBUTION STATEMENT (of this Report)

This document has been approved for public release and sale; its distribution is unlimited.

12 79p.

17. DISTRIBUTION STATEMENT (of the abstract entered in Block 20, if different from Report)

9 Final rept. Oct 77- Oct 78

18. SUPPLEMENTARY NOTES

19. KEY WORDS (Continue on reverse side if necessary and identify by block number)

Electro-Optical, Contouring, Helicopter Rotor Blades

in.

20. ABSTRACT (Continue on reverse side if necessary and identify by block number)

Non-contact contour measurements of helicopter rotor blades to accuracies of 0.001" are possible via range finding by triangulation employing electro-optical techniques. A laboratory breadboard of such a system has been built and tested. The results of these tests indicate that the construction of a full prototype system is feasible and desirable.

DD FORM 1 JAN 73 1473 EDITION OF 1 NOV 65 IS OBSOLETE

SECURITY CLASSIFICATION OF THIS PAGE (When Data Entered)

new

4 11 251

This project has been accomplished as part of the U.S. Army Materials Testing Technology Program, which has for its objective the timely establishment of testing techniques, procedures or prototype equipment (in mechanical, chemical, or nondestructive testing) to insure efficient inspection methods for materiel/material procured or maintained by DARCOM.

TABLE OF CONTENTS

LIST OF ILLUSTRATIONS

LIST OF TABLES

LIST OF TABLES

1. SUMMARY

Dreyfus-Pellman Corporation (D-P) was awarded Contract DAAK-50-78-C-0008 (P6D) to accomplish the Phase I portion of a two-phase program. This two-phase program will result in a prototype, computer controlled, non-contacting electro-optical system to measure the contour of helicopter rotor blades.

This report covers Phase I only. The effort called for by Phase I was intended to prove the feasibility of Dreyfus-Pellman's concept. During Phase I a preliminary design of the overall system was completed, and an experimental model of the Electro-Optical Range Finder was designed, fabricated, and tested.

The final system will permit the contouring of an entire helicopter rotor blade in 30 minutes by electro-optical techniques without contact between contouring equipment and the surface being measured. The contouring system elements can be several feet from the surface being contoured.

The entire operation is under computer control and fully automatic. It can be changed by reprogramming to contour a wide variety of surface shapes. Expensive tooling need not be fabricated for each part being contoured.

Operator skill needed is minimal as all functions are under computer control.

Output format can be varied to suit the individual user.

This report describes the Phase I effort. The results of tests performed by Dreyfus-Pellman show that all objectives were achieved. The concept is valid; contour measurements can be made to accuracies in the order of $\pm$ .001" in a factory environment.

To test contouring accuracy, measurements were made electro-optically at eighty-seven points on the surface of four sample helicopter rotor blades including the area of the leading edge. In order to check the accuracy of these non-contact electro-optical contour measurements, mechanical contact gage measurements were also made on the same sample rotor blades. The differences between electro-optical measurement and mechanical measurement averaged 0.0014" in Y (the direction of chord thickness) and .0042" in X (along the blade chord). However these differences are not accurate representations of the errors in the electro-optical measurement system, because the method of analysis assumed that the exact same point had been measured both mechanically and electro-optically whereas experimental constraints had limited point-matching accuracy to $\pm$ .005" in X. Approximately ninety percent of the difference is attributed to point-matching displacements and

to inaccuracies in mechanical measurement. The electro-optical contour measurements were repeatable to 0.0001" in both X and Y. In order to compare the electro-optical measurements to a known standard, contouring test measurements were made on a precision-ground cylinder of known diameter. These measurements show a standard deviation of contouring accuracy under 0.0002". They also show repeatability in the electro-optically measured cylinder radii of 0.0001".

Contouring test measurements were also made on partially-painted translucent fiberglas and black rubber coated rotor blades in order to determine how light penetration at the rotor surface and low reflectance would affect contour measurement. These measurements show that the electro-optical contouring system gives accurate results on both painted and unpainted fiberglas as well as on rubber. The data does, however, show a slight reduction in contouring accuracy on unpainted fiberglas.

Photometric measurements were made on the angular reflectivity of a wide range of rotor materials supplied by helicopter manufacturers. The materials included various composite plastics, painted and unpainted fiberglas, matte aluminum, and graphite. Measurements were made at various orientations and locations corresponding to the full range of rotor surface conditions anticipated. The results of these tests showed that the system for electro-optical contouring will work on all of the materials tested. Photometric tests on supplementary non-rotor materials showed that limitations would be encountered in contouring polished metal surfaces with surface roughness smoother than approximately 16 microinches rms.

The detailed test data summarized above is included in this report, as are descriptions of the testing procedures and analyses of the results.

1. BACKGROUND

The aerodynamic characteristics of main rotor blades of helicopters has always been considered a critical parameter by the industry. One of the major manufacturing problems has been to accurately determine the as-built configuration. There have been three basic measuring methods used typically; mechanical, electro mechanical and pneumatic mechanical. In most cases these methods are constrained in application to predetermined chordal stations, and the measuring devices are moved from point to point along the span of the blade. The number of data points has been limited and the amount of time required to take the measurements is relatively long. There is significant concern in the industry regarding the correlation of as-built configuration and performance. There are schools of thought that feel by knowing more about the surface condition of the blade and by having better data to relate to theoretical airfoil it may be possible to relax manufacturing tolerances without sacrificing performance. The result would be the availability of a comparatively less expensive blade.

These types of measurement equipment are subject to frequent failure. The two predominant modes are total malfunction and inaccurate data. As a result of these frequent problems, the equipment requires reasonably high investment and maintenance costs. In many cases the data derived from these measurement devices are not easily coupled to any form of computer. It has long been the desire of the industry to have fast, accurate measuring equipment easily adjustable to any number of data points along the chordal dimension in conjunction with the data processing capability that provides a summary assessment of the surface of the blade. An additional characteristic that is needed, is a measurement device with the versatility of accommodating various sizes of blades and airfoil shapes without the necessity of complete and extensive retooling. The D-P electro-optical measuring concept offers a promising solution to these problems. It is capable of measuring any form of airfoil; it can be programmed to provide almost an infinite number of measurements along the chord and the span of the blade. The resulting signals from the measuring devices are easily converted to a form usable in a basic computer, thereby allowing comprehensive assessment of the as built configuration covering all parameters such as camber, twist, waviness, chordwise bow, and spanwise bow. In addition, contour measurements will be made in the area of and at the leading edge.

2. ADVANTAGES DERIVED FROM THIS TECHNIQUE OF CONTOUR MEASUREMENT

The Noncontacting Electro-Optical System to automatically measure the contour of helicopter blades designed by Dreyfus-Pellman Corporation is based upon solid highly reliable, proven electro-optical components and engineering practice. A breadboard of the Electro-Optical Range Finder which is the heart of the proposed system was built, tested and demonstrated under Contract DAAK 50-78-C-0008 (P6D) with the Army Aviation Systems Research and Development Command. The tests performed under this Contract and the analysis made show that the accuracies described, i.e. $\pm$ 0.001" can be met in a reasonable and practical way. The system's design utilizes these components in such a manner that the requirements imposed upon the associated mechanical structure are reduced by an order of magnitude over conventional electro-mechanical contacting measuring machines.

The combination of the electro-optical subsystem with modern electronic data processing components results in a powerful flexible system that can be used in a factory and/or engineering environment to perform measurements on helicopter rotor blades to an accuracy and with speed which represent an advance in the state of the art.

If one were to build conventional equipment employing contact probes or proximity probes to make the required contour measurements, the accuracy of these measurements would depend upon the stability of the mechanical structure which serves as a reference. Any twisting, bending or settling of the structure after calibration or during measurement would affect the accuracy of the machine. Probes must cover over 40 feet spanwise and 48 inches chordwise with a positional accuracy of better than $\pm$ .001 inch under normal shop conditions. The cost and complexity of a mechanical X-Y carriage positioning a probe with this accuracy is extremely high. If multiprobes are used, the relative position of one to the other must be known and held to better than $\pm$ .001"; this also is expensive.

In addition, conventional equipment affords little or no flexibility in operation. Once the probes are positioned for a certain type of blade,

rearrangement which can be costly is required before any other size blade can be measured. The proposed system need not be rearranged. All that is required is operator control or reprogramming for automatic measurement.

The use of the proposed machine to measure rotor blade contour will enable helicopter manufacturers to:

1. Improve vehicle performance.

2. Reduce vibration so that the helicopter would be a better platform for the payload. This would enhance payload performance and extend payload operating life.

3. Reduce vibration so that rotor and gear box life would be extended.

4. Reduce flight test for rotor blade tracking problems.

As to factory environment, our design offers the following advantages over conventional mechanical or electro-mechanical contacting systems:

1. Lower operating cost because set up is simple. Physical changes and calibration are not required for each blade type measurement. Changes are made via programming quickly and economically.

2. The mechanical structure is less costly than conventional structures because the requirements for dimensional stability are reduced by an order of magnitude due to the self-calibration features of our design and the fact that the balanced rotary motions of the scanner will cause less deflection than the linear motion of conventional contacting probes.

3. Probe wear together with the cost of probe replacement is eliminated as our system is noncontact.

4. Quick and automatic calibration. Reference points can be scanned between each blade measurement in order to calibrate and establish a reference coordinate system from which each blade measurement can be taken. In addition, reference calibration is achieved between each chordwise scan.

5. High thruput. Measurements are fast. Thirty minutes for an entire rotor blade.

6. Compatible with modern data processing systems. Outputs can be tailored to meet the desired output format. Summary data and analysis can be made quickly and economically.

7. Measurements can be made in the area of and at the leading edge.

The Dreyfus-Pellman system utilizes proven technology; the application of this technology was successfully demonstrated during the first phase of this program.

3. AERODYNAMIC AND MANUFACTURING CONSIDERATIONS

Dreyfus-Pellman's coordinate measuring machine will provide a blade contour measuring system, which will be accurate and rapid, providing blade measurement data to the operator in a matter of seconds by the use of a minicomputer and a high speed printer. The data will provide a binary indication of acceptability. When the blade is unacceptable, it will specify the exact parameter and where applicable the chord and spanwise location.

For example, the computer will provide for typical blade contour readings at spanwise locations of 20%, 40%, 60%, 75%, 90%, and 95% of blade span. At each spanwise station readings will be taken at the leading edge and of the chord height at each 5% of the chord up to and including the 50% chord length and each 15% of the chord for the remainder of the chord length. The readings will be taken simultaneously of the top and bottom of the blade providing a total of 168 data points.

The computer will calculate top and bottom chordal heights and a print out will provide chordal actual heights and any deviations from requirements. The system will be designed so that easy alteration of the standard measurement points can be achieved. This provides the capability of using the system as an analytical tool for evaluating specific aspects of the blade manufacturing tooling reproducibility. It may also be used to evaluate local areas of the blade with regard to comparisons of as built configurations to aerodynamic performance.

Utilizing the actual dimensions airfoil waviness and camber of the airfoil at each spanwise station will be calculated and summarized. Additionally during the course of scanning the blade contour, at the various spanwise stations, the twist of the blade will be calculated and printed out as a part of the data.

Using the aforementioned summary numbers and the blade twist, the computer will calculate and print out the trim tab angular adjustment that will be required to cause the blade to track when installed on an aircraft.

The equipment will provide a structure to facilitate insertion and removal of the blade. It will be front loaded in a manner that will minimize the need for clearance area around the system.

4. SPECIFIC ACCOMPLISHMENTS

Dreyfus-Pellman was awarded Contract DAAK 50-78-C-0008 (P6D) which covered the first phase of a multi-phase program to design, build, test, and install a machine to automatically measure the contour of helicopter rotor blades using non-contacting electro-optical techniques.

The work performed under this contract indicates that the engineering design concept employed by Dreyfus-Pellman Corporation is sound and will result in a machine meeting the performance goals stated in Section 5 of this report. Test results are shown in Section 9.

During Phase I of this program, Dreyfus-Pellman Corporation:

1. Completed the Preliminary Design of the overall system.

2. Designed, built and tested a breadboard Electro-Optical Range Finder using actual helicopter rotor blade sections constructed of various material and of several sizes.

3. Completed the Preliminary Design of the Electronic Data Processing System.

4. Completed the Preliminary Design of the Overall Structure.

Figures 1, 2, and 3 are photographs of the breadboard system.

During Phase I, an angular readout system was designed and calibrated to accuracies of less than 1 second of arc. This system, when coupled with electro-optical detectors, is able to detect contour changes in rotor blades as low as 0.000050" and exhibits sufficient stability to permit us to predict with confidence that the full prototype system is feasible and practical.

From an economic and practical engineering standpoint, it follows that the work begun in Phase I should continue and will result in usable factory hardware.

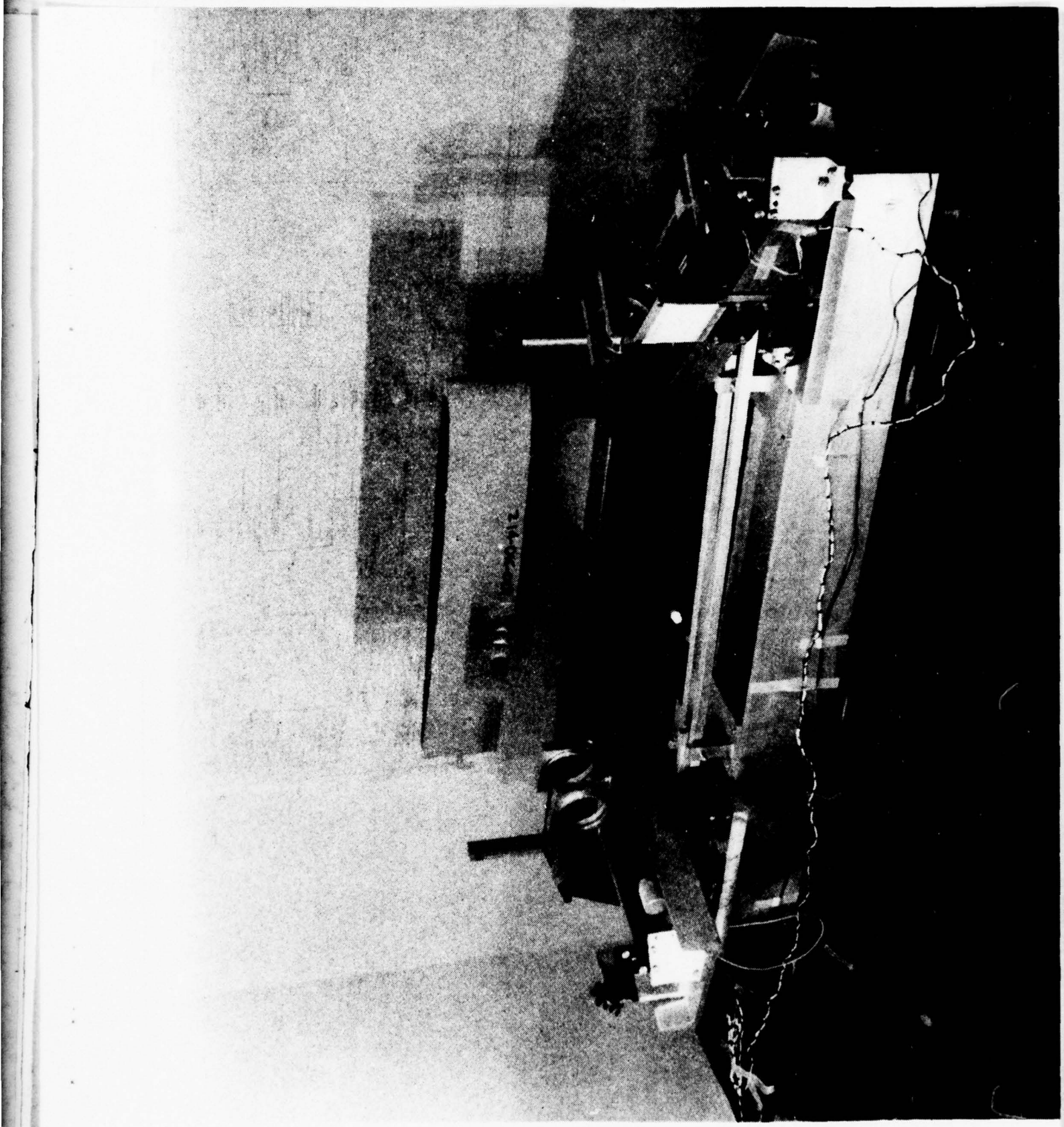

RANGE FINDER BREADBOARD SYSTEM

FIGURE 1

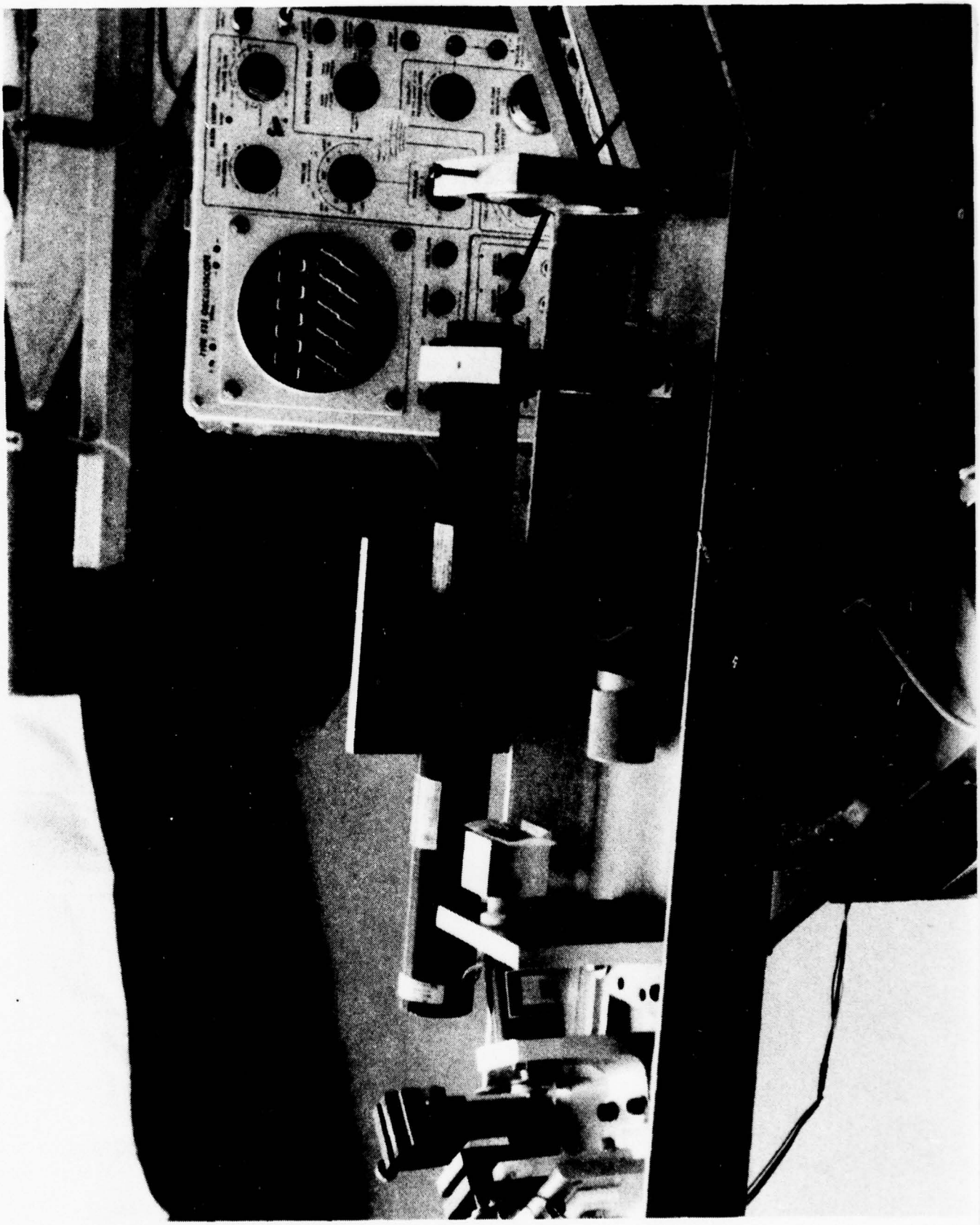

ILLUMINATOR ASSEMBLY

FIGURE 2

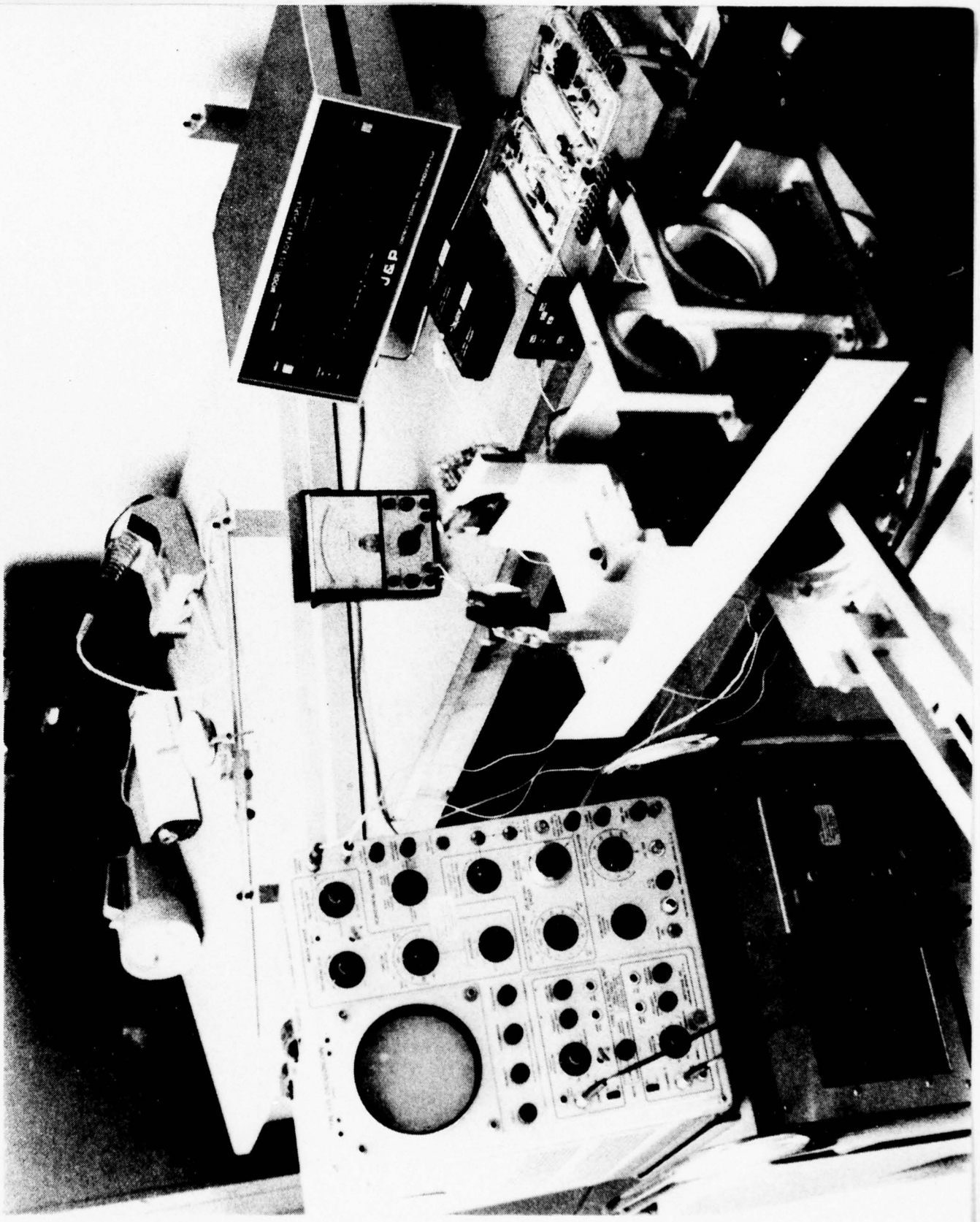

TRACKER ASSEMBLY

FIGURE 3

5. PERFORMANCE GOALS

The prototype rotor blade measuring machine which Dreyfus-Pellman Corporation initiated shall be designed to meet performance goals which are based upon manufacturing and engineering requirements which will be encountered over the next ten years.

The final machine will work in conjunction with electronic data processing equipment which will afford a high degree of flexibility. Changes in measuring requirements will be accomplished largely through the use of programming. Mechanical changes to the machine will be held to a minimum. In most cases the only mechanical change required will be modification or adjustments to the holding fixture to accommodate different size rotor blades. The machine will be designed to provide a high degree of accuracy without any loss of reliability. As a goal, the machine will make the following measurements to the accuracies specified:

1. The primary function and most important objective of this equipment is to measure cross-sectional shape of blades and blade spars. The absolute accuracy of the blade contour relative to a reference plane shall be 0.001". Based upon the contour map of the blade obtained by scanning the cross-section of the blade including the leading edge at various stations waviness, camber, flatwise bow, edgewise bow and twist are to be computed. Accuracy for twist shall be one minute of arc and accuracy for flatwise and chordwise bow shall be 0.010".

2. The machine shall have the capability of making measurements as close as 0.010" apart on certain portions of a chordwise scan (for example at the leading edge). The time constant of the measuring system shall be short enough to permit many measurements to be made in critical areas without slowing down the overall measuring cycle. The number of measurements shall be controlled from a keyboard.

3. The dynamic range of the measuring system shall be great enough to accommodate different blades where the measurement surfaces will vary in location (one from the other) by as much as 5 inches.

4. Spanwise movement along the blade shall be accomplished by automatically moving the carriage of the measuring system. The blade shall remain stationary. Spanwise location of the measuring device shall be automatic based upon preprogrammed inputs to the machine.

5. A keyboard shall permit the operator to select spanwise position in the event that preprogrammed positions are not desired or if additional positions are desired. When operating in the preprogrammed mode, the machine will automatically move to the next spanwise position at the completion of measurement of the chordwise contours. Spanwise location shall be accurate to 0.030" of true position.

6. A self calibration feature shall be incorporated into the machine. Calibration shall be checked at the beginning and end of each chordwise scan. The computer system will adjust all readings to account for the calibration inputs.

7. The machine shall accommodate rotor blades having a chord width as large as 48", a span as long as 40', and thickness changes per side as great as 3".

8. The measuring speed of the system shall be such that at least 4000 points may be measured on a 40' rotor in 30 minutes.

6. SYSTEM DESIGN

Introduction

Dreyfus-Pellman Corporation's design utilizes noncontacting electro-optical sensors in a triangulation range finder arrangement to measure the contour of helicopter rotor blades. Two such range finders are used so that both sides of the rotor blades can be measured simultaneously. The two sides of the blade are related in a measurement sense, by having common reference points adjacent to the leading and trailing edge measured by both range finders. The use of a small mirror near the leading edge affords a proper viewing angle for this portion of the blade.

Figure 4 shows the contemplated design of the overall system. It is an artist's conception based upon the preliminary design of the structure discussed in Section 7 of this report.

The mechanical structure of the complete measuring system consists of two main sections.

The first section is a fixture which supports the blade being measured. This fixture locates the blade on two reference chords which establish the coordinate system for contour measurement. In addition, optical references are incorporated into this fixture so that the optical sensor will always look at these references when measuring surface contour (Figure 5). That means that the position of the optical sensor need not be controlled to plus or minus .001" relative to the rotor blade but that its position be known to plus or minus .001" as determined by scanning the reference bars. This reduces its structural complexity by an order of magnitude.

The second section of the structure is a transporting mechanism which moves the optical sensor spanwise over the blade being measured. The chordwise scanning motion is generated by rotating the illuminator and tracker through sufficient angles to scan the entire chord. In view of the fact that the exact position of the optical range finder is determined by a physical reference tied to the holding fixture, its position need not be

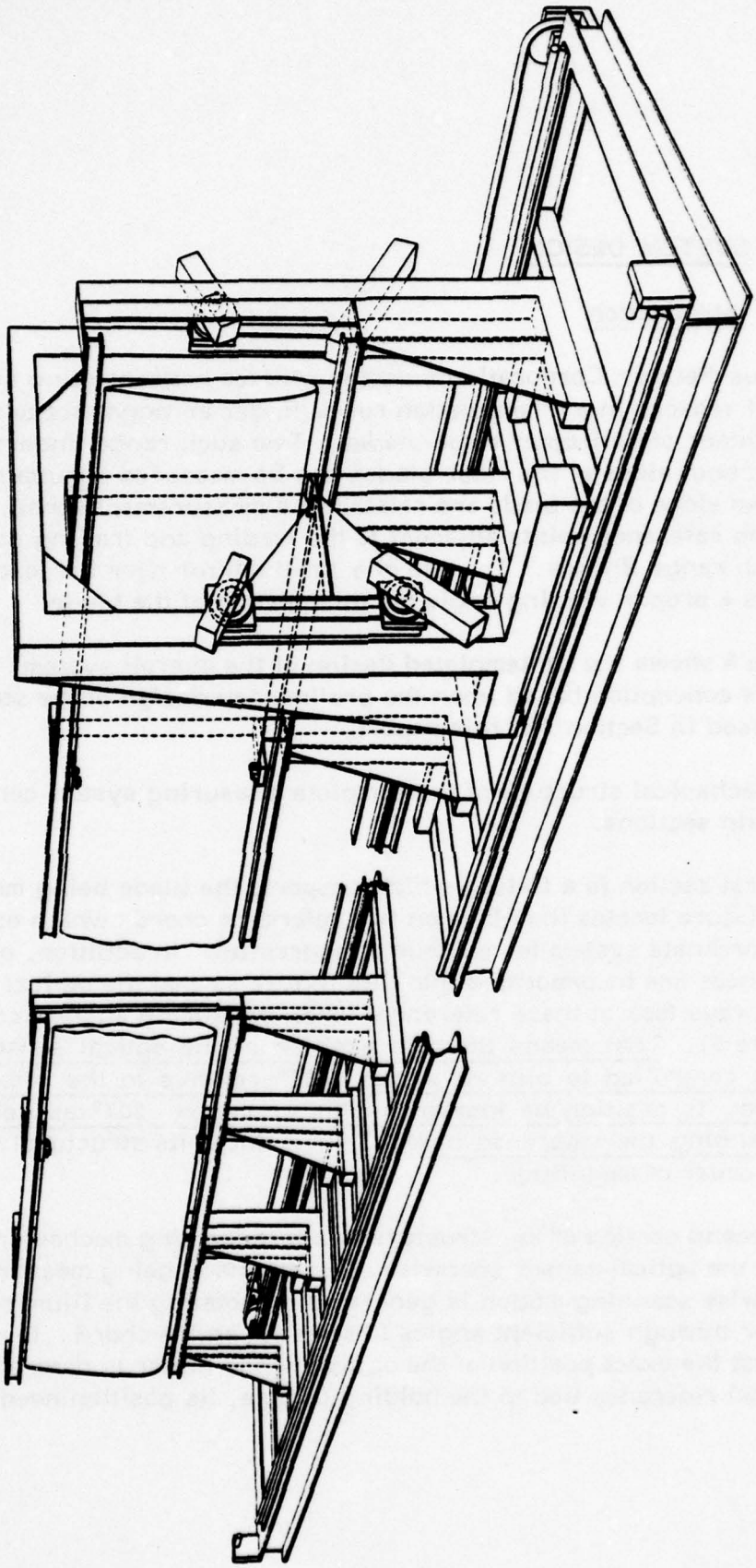

FIGURE 4

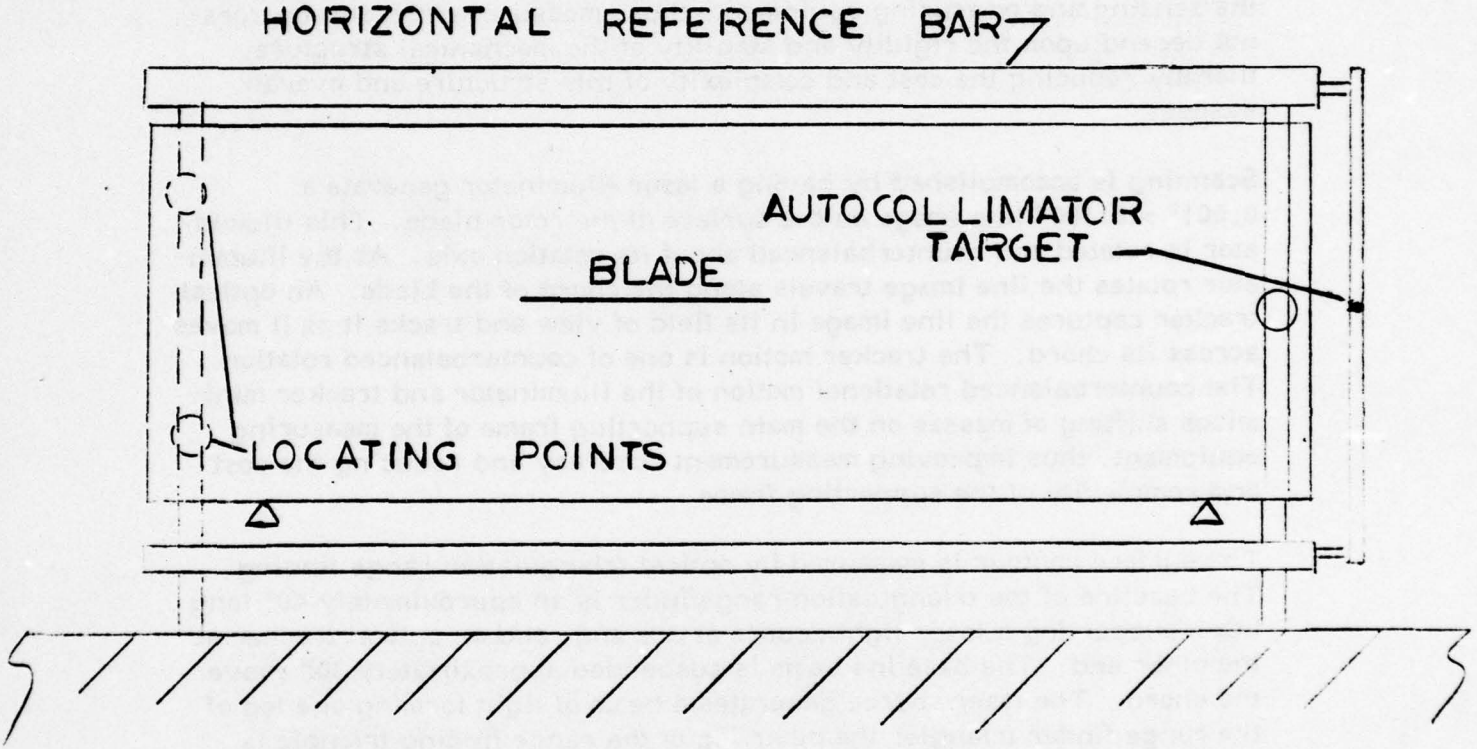

HOLDING FIXTURE

FIGURE 5

controlled to a high precision. However, its position must be known accurately. This noncriticality of position reduces the cost and complexity of the transporting mechanism. In addition, by isolating the holding and reference fixture from its moving transporting system, its complexity and cost is reduced (Figure 6). The salient feature of this system is that most of the problems associated with mechanical or electromechanical contactors and precision X-Y carriages are avoided. Optical references are established and maintained independent of the structure which carries the sensing and measuring equipment; thus, measurement accuracy does not depend upon the rigidity and stability of the mechanical structure, thereby reducing the cost and complexity of this structure and overall system.

Scanning is accomplished by having a laser illuminator generate a 0.001" x 0.100" line image on the surface of the rotor blade. This illuminator is rotated and counterbalanced about its rotation axis. As the illuminator rotates the line image travels along the chord of the blade. An optical tracker captures the line image in its field of view and tracks it as it moves across its chord. The tracker motion is one of counterbalanced rotation. The counterbalanced rotational motion of the illuminator and tracker minimizes shifting of masses on the main supporting frame of the measuring equipment, thus improving measurement accuracy and reducing the cost and complexity of the supporting frame.

The surface contour is measured by optical triangulation range finding. The baseline of the triangulation rangefinder is an approximately 40" long beam supporting a laser light source at one end, and an optical tracker at the other end. The baseline beam is suspended approximately 30" above the chord. The laser source generates a beam of light forming one leg of the range finder triangle; the other leg of the range finding triangle is generated by the axis of the optical tracker. The location of the contour point at the apex of the triangle is then defined by angle, side, angle (illuminator angle, baseline, and tracker angle), and can be trigonometrically calculated.

In order to contour the surfaces, the illuminator pivots so that the laser spot travels across the chord at an angular rate of 3^{o}/second. As the illuminator beam pivots, the tracker pivots to track the laser spot under closed-loop servo control, so that the intersection of the illumination axis and tracker axis maps the surface contour. This is accomplished to an accuracy of 0.050". An open loop sensor located in the tracker determines the position of the laser spot to an accuracy of .0005" (Figure 7).

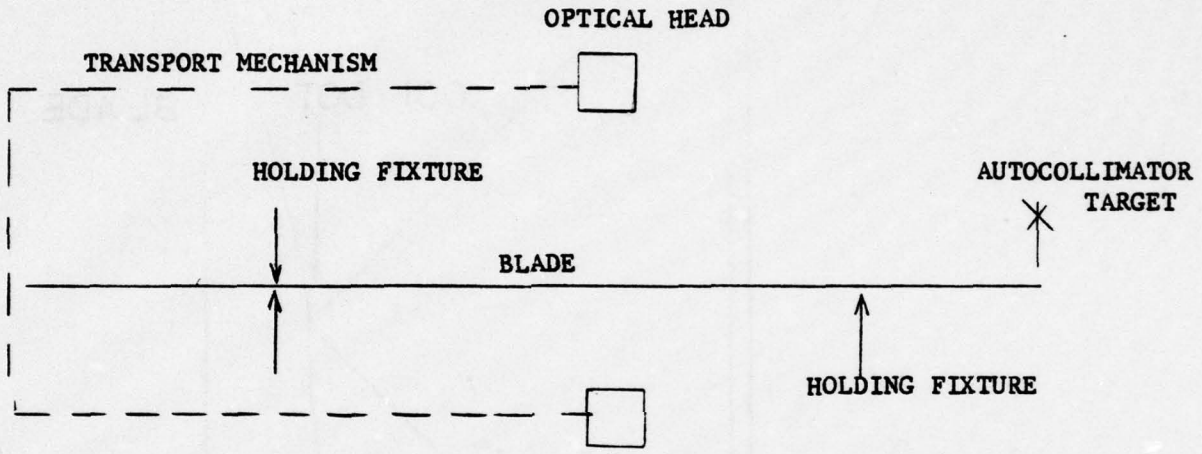

TRANSPORTING MECHANISM

FIGURE 6

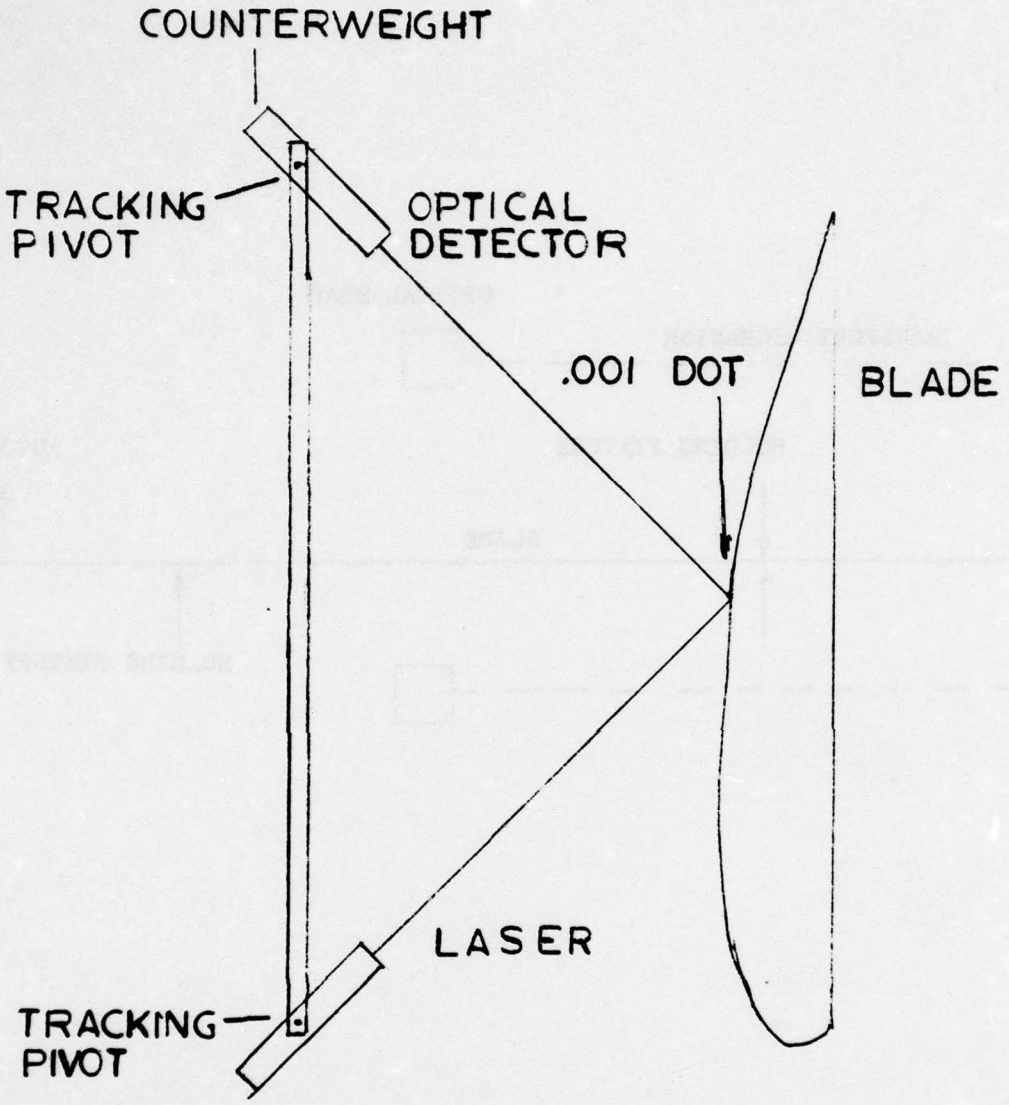

RANGE FINDER

FIGURE 7

The laser beam is modulated at a frequency of 1 kilohertz, and the optical tracker is filtered in the spectral (wavelength), temporal (frequency), and spatial (field of view) domains to prevent ambient stray light from biasing the contour readings.

As the laser illuminator pivots, its beam is kept focused on the surface of the rotor blade by a closed-loop, focusing adjustment on its output lens. The tracker is likewise focused.

The range finder assembly travels intermittently along the surface's long dimension from measuring station to measuring station. As it travels, the 50' long span girder will tend to settle and twist. Therefore, at the beginning and end of each pivoting scan of the contour, the range finder is calibrated by locating two reference points located near the leading and trailing edges of the surfaces on the holding fixture. The angular orientation of the pivot axis is monitored by an autocollimator connected rigidly to the pivot axis which is looking at a fixed target on the holding fixture.

Range Finder

The range finder consists of two optical assemblies: a laser illuminator and a contour tracker, which are located at the ends of a 40" long baseline beam. The baseline beam is oriented approximately 30" away from from and parallel to the rotor chord, and perpendicular to the span axis. The illuminator and the tracker are supported on pivot axes and toed-in so that their optical axes intersect at the rotor surface. The illuminator generates a .001" x .100" line of laser light on the rotor surface with its long axis parallel to the rotor span axis. The illuminator pivots at an angular rate of 3 degrees per second, sweeping the line of light across the surface of the rotor. As the illuminator pivots, the tracker also pivots smoothly under computer control, to follow the line of light across the rotor surface. Residual tracking errors due to unpredicted surface contour variations are measured by an open-loop sensor in the optical tracker to an accuracy of $\pm$.0005" over a range of $\pm$.0500".

The laser illuminator contains a helium-neon laser emitting 5 milliwatts of polarized light at 0.63282 micron wave length in a 0.8 mm diameter beam

with 1 milliradian beam divergence. The light path is folded by flat mirrors for system compactness and its diameter is expanded sixty times by an optical beam expander in order to reduce its divergence from 1000 microradians to 25 microradians in the direction perpendicular to the rotor span axis. In the direction parallel to the span axis, a hundred times larger beam divergence of 2500 microradians is generated by a cylindrical lens incorporated in the beam expander. The expander output is focused on the rotor surface by a servoed objective lens so that it generates a .001" x .100" line image.

The contour tracker views the illuminated line on the rotor surface through a lens system consisting of a collimating objective lens and a servoed focusing objective lens. In the space between these two lenses, a square aperture stop is located with one pair of sides parallel to the line image on the rotor surface. This square stop (operating in conjunction with the two lenses near it) generates a square pyramid of light flux in the tracker. This pyramid converges toward a line-shaped apex parallel to the same two sides of the aperture stop; the apex is an image of the laser line on the rotor surface.

The square pyramid of light is intercepted near its apex by a two-element silicon photodetector. The intersection of the photo detector plane with the flux pyramid is a rectangle of light with an intensity distribution which is bilaterally symmetrical. If the laser line moves off center in the field of view of the tracker, the difference of the flux levels intercepted by the two silicon elements is a direct linear measure of the distance of the laser line from the center of the tracker's field of view.

The optical geometry and detector configuration described above are key elements in this system. Its metrological integrity depends on the feasibility of establishing a stable relationship between the flux difference on the two detectors and the laser line position. We have selected a two-element silicon photo detector because these detectors exhibit responsivities which change only about 0.1%/C^{o}. Furthermore, these two-element silicon detectors are made as a unit; hence the individual detector elements have practically identical chemical and physical properties, and tend to track their cellmates in photo-detective responsivity. By way of comparison,

photomultiplier detectors have responsivities which change approximately 1%/C° and are individually made; hence it would be difficult to get two photomultipliers to match in responsivity over the temperature range and effective operating lifetime required in this type of application.

7. MECHANICAL DESIGN

Introduction

During Phase I of the program, Dreyfus-Pellman Corporation completed the preliminary design of the overall system. The overall size of the machine is approximately 50' long, 10' high, and 8' wide. (See Figure 4.)

This design incorporates the following concepts:

1. Base - The base is designed in sections to allow use of reasonable stock length of structural material, be transportable and allow installation within reasonable building structures. It has appropriate means for connecting sections and for leveling its entire length.

   The base contains the mounting for the carrier track, track leveling mechanism, and mounting pads to align and secure uprights.

   The base has its portion of the drive mechanism needed to advance the carrier and the encoder drive for position determination.

   The base has a device (trough or similar) to contain wires and cables trailing the carrier when in motion, and the base and carrier track are of suitable length to roll the carrier clear for loading and unloading test samples.

2. Uprights - The uprights each have a bottom section matching the base upright mounting and leveling pads.

   The number of uprights and their spacing is adequate to support the reference bars and the test sample.

   The uprights contain fixed mounting pads for the lower reference bar and test sample lower nest, adjustable mounting pads for the upper reference bar and test sample upper nest and securing device.

The width of the uprights is minimized, within structural strength limitations, to allow maximum test sample exposure for inspection.

3. Carrier - The carrier is a gantry type having a two-wheel device on one side and one-wheel device on the other to provide a stable three-point suspension.

   The carrier contains its portion of the drive mechanism and encoder affixed to its two-wheel side.

   Each of the two vertical sections of the carrier contains mounting pads to hold the scanning devices.

   All wire and cabling depart the carrier from the two-wheel side to prevent misalignment of the carrier on its track.

   Carrier travel is sufficient to allow loading and unloading of test samples when in home position.

8. ELECTRONIC DATA PROCESSING

Introduction

The electronic data processing subsystem was configured during Phase I of the program; the choice of system design was made with the assistance of Hughes Helicopter, taking into account the data processing requirement of a major helicopter manufacturer. The computer and peripherals chosen provide a system that will:

1. Perform the computations to measure the specified dimensions;
2. Be easy to use;
3. Be low in cost;
4. Provide flexibility as requirements change.

The system is sufficient to develop, modify and execute the required measurement programs and calibration programs.

The computer subsystem has the following features:

1. Capability of modifying existing or generating new measurement programs;
2. Capability of storing several measurement programs;
3. Operation communication through keyboard;
4. A programmer trained in the use of FORTRAN shall be able to reprogram the computer;
5. Output will be printed on any desired format of 80 characters per line;
6. Printing time is 8.3 seconds per line.

Description

The Electronic Data Processing System, EDPS, consists of the following major items:

1. A general purpose microcomputer with sufficient speed and memory to handle all of the control functions of the measurement system as well as the computational and report generating functions. In addition, the EDPS will contain all necessary hardware and software to develop and/or modify the measurement programs supplied with the systems.

2. Dual floppy disk system. This subsystem provides ample non-volatile storage for measurement programs, blade specification data, and general purpose utility programs. Two independent disk drivers are supplied so that disks may be copied for back-up and to lessen the risk of downtime due to hardware failure.

3. Punch card reader for standard 80 column 12 level punched cards.

4. Interface for #3. This vender-designed module interfaces the card reader to the computer and will reside within the computer chassis.

5. Terminal - A compatible send/receive Keyboard/Printer. This terminal is used for all program development and maintenance, as well as report printing during blade inspection. Also certain operator input and requests are entered via the terminal's keyboard.

6. Interface for console electronics - will reside within computer chassis.

7. Interfaces for the illuminator and trackers. These will be designed to plug into the computer chassis. They will allow the computer to control scan position and velocity, focus for both the illuminator and the tracker, and read exact illuminator and tracker angular position. In addition, tracker error values are made available to the computer via these interfaces.

8. Interface for the carriage drive motor and carriage position reader.

Software

The measurement programs will be written FORTRAN IV with the time critical positions written in assembly language. FORTRAN was chosen because:

1. It most easily handles the computational function and the formatted printer output.
2. It is a well-known computer language.
3. It is compact and easy to read and understand.
4. It requires a much shorter development cycle.

9. TESTS

This section shows the results of the tests performed on the experimental model Electro-Optical Range Finder. These tests covered both accuracy and repeatability as well as applicability of the system to measure contours of blades made of various materials.

Accuracy and Repeatability

In order to check the accuracy of the electro-optical contour measurements, mechanical contour measurements were also made on the same sample rotor blades. The differences between electro-optical measurement and mechanical measurement taken over 87 contour points averaged 0.0014" in Y (chord thickness) and 0.0042" in X (along the chord). A close look at the test set up particularly in the area of mechanical measurements leads us to believe that the mechanical measurements are less accurate than the electro-optical measurements. In particular, the mechanical gauges have scribe marks every 0.001 of an inch and interpolation is required to obtain 0.0001" readings. It was also required that identical points be measured mechanically and electro-optically. This required setting a 1/16" diameter ball on the dial indicator to the same point as a 0.001" diameter laser spot by eye. Errors in doing this are considered to be as much as 0.005" in X. Approximately ninety percent of the difference can be attributed to inaccuracies in mechanical measurement. Repeatability of the electro-optical contour measurements is better than 0.0001" in both X and Y.

These results show that the concept is viable and that a prototype system employing the Dreyfus-Pellman concept is reasonable and will result in accurate economical contour measurements of helicopter rotor blades.

Definition of Terms

N Distance in centimeters, along the blade surface, from the leading edge to the point where coordinates were measured both electro-optically and mechanically

IL Illuminator Angle in degrees

TR	Tracker Angle in degrees
XM	Vernier Caliper reading in inches
YM	Dial Indicator reading in inches
BLC	Corrected Baseline in inches
XEOD	Electro-Optical X coordinate in direct view coordinates
YEOD	Electro-Optical Y coordinate in direct view coordinates
XEOM	Electro-Optical X coordinate in mirror view coordinates
YEOM	Electro-Optical Y coordinate in mirror view coordinates
α	Slope of rotor blade at point being measured as related to mechanical measurement system
YMC	Y mechanical coordinate corrected for local slope
XMT	XM translated to electro-optical coordinate system
YMCT	YMC translated to electro-optical coordinate system
XMTR	XMT rotated to electro-optical coordinate system
YMCTR	YMCT rotated to electro-optical coordinate system
IOT	Inductosyn offset angle - Tracker
IOI	Inductosyn offset angle - Illuminator
TRC	Corrected tracker angle
ILC	Corrected illuminator angle
ET	Tracker eccentricity

XΘ	X coordinate about which rotation occurs
YΘ	Y coordinate about which rotation occurs
X↕	X coordinate being rotated
Y↕	Y coordinate being rotated
Θ	Angle of coordinate rotation
XE	XMTR - XEOD or XMTR - XEOM
YE	YMCTR - YEOD or YMCTR - YEOM
I	Intersection of Illuminator optical spindle axis with baseline
T	Intersection of Tracker optical spindle axis with baseline
t	X coordinate of intersection of Tracker optical spindle axis with baseline
S	Illuminated point on leading edge
M	Point on the mirror surface through which the chief ray of the Tracker views S
AI	Baseline for mirror triangulation
AI'	Corrected baseline for mirror triangulation

Test Set Up - Description

General Discussion

The test set up consisted of an Electro-Optical Range Finder functionally and geometrically equivalent to the one which will be used in the prototype system and a mechanical X-Y coordinate measuring device. The coordinates of points as close to identical as possible were determined both electro-optically and mechanically and then compared. The differences between the electro-optical coordinates and mechanical coordinates were then called the measurement error. This is really a measurement difference and can be attributed to errors in electro-optical coordinate measurement, mechanical coordinate measurement or a combination of both. A close look at the test set up particularly in the area of mechanical measurements leads us to believe that the mechanical measurements are less accurate than the electro-optical measurements. In particular the mechanical gauges have scribe marks every 0.001 of an inch and interpolation is required to obtain 0.0001" readings. It was also required that identical points be measured mechanically and electro-optically. This required setting a 1/16" diameter ball on the dial indicator to the same point as a 0.001" diameter laser spot by eye. Errors in doing this are considered to be as much as 0.005" in X.

Electro-Optical Range Finder

The Electro-Optical Range Finder consists of an Illuminator and a Tracker separated by a 40" baseline. A 0.001" Dia spot is projected onto the surface of the rotor blade section. Where this is done the angle which the Illuminator makes with the baseline is measured to an accuracy of 0.0001^{o} using an inductosyn. The Tracker is positioned so that the 0.001" Dia spot on the rotor section is central to its optical axis to within 0.0001^{o}. This is accomplished through the fine tracker circuitry and read using an Inductosyn. The point coordinates are then determined by solving the triangle produced by the baseline, Illuminator optical axis and Tracker optical axis.

Mechanical Coordinate Measurement

The mechanical set up consists of a 2" range, 0.001" accuracy dial indicator mounted orthogonally to the moving jaw of a 24" caliper. This device is then mounted rigidly to the frame holding the rotor section and mechanical coordinates are measured. Corrections are made to account for probe shape where applicable.

Leading Edge Measurement

In order to measure the leading edge of the blade section, a mirror is employed so that the Tracker can "see" the illuminated spot in the area of and at the leading edge. Illumination is direct.

Coordinate System Definitions

There are five X-Y coordinate systems used when making the necessary measurements. These are:

1. Electro-optical Direct reading
2. Electro-optical Mirror reading
3. Mechanical for correspondence to Electro-optical Direct reading
4. Mechanical for correspondence to Electro-optical Mirror reading
5. Mechanical for correspondence to Electro-optical Direct reading Tail Section of Long Rotor Blade. This coordinate system is required because the 24" vernier caliper will not permit coverage of a long rotor blade section in one set up. Figure 8 shows the relationship between the various coordinate systems.

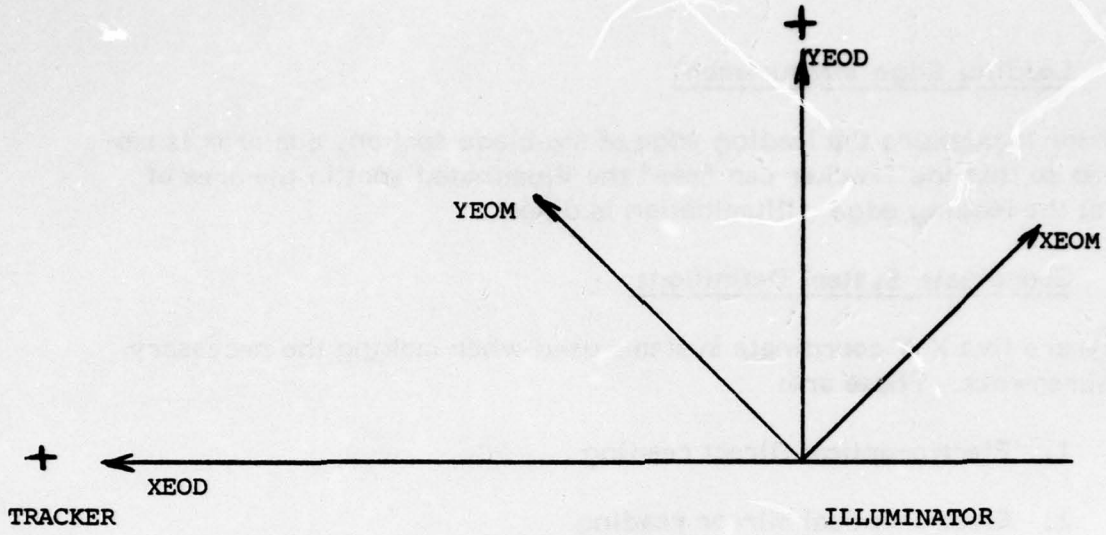

ELECTRO OPTICAL COORDINATES

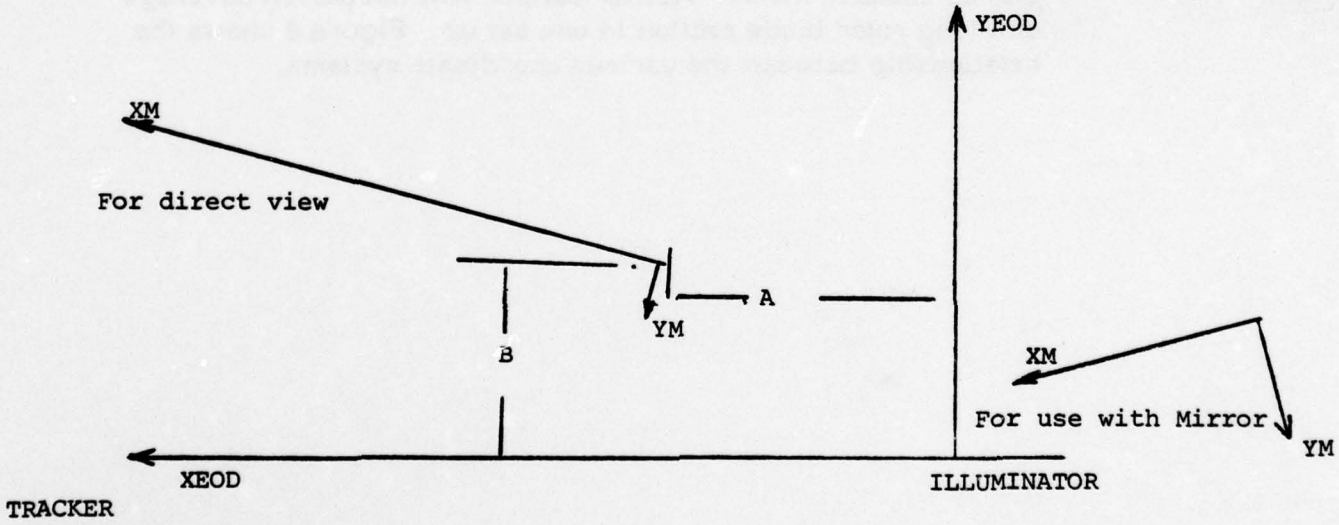

MECHANICAL COORDINATES

COORDINATE SYSTEMS

FIGURE 8

Data Taking

The following data is taken for each point where coordinate determination is required:

1. IL
2. TR
3. XM
4. YM

In order to demonstrate the repeatability of the Electro-Optical System, 1 and 2 above were repeated for selected direct view blade sections.

Data Processing

The following describes the calculations required to convert the data taken above into usable coordinate information from which contour differences between electro-optical and mechanical coordinate measurements can be determined.

XEOD and YEOD Calculations

Calculation of XEOD and YEOD for all points taken by the electro-optical system directly (i.e. not using the leading edge mirror) is as follows:

Figure 9 shows the geometry of the electro-optical coordinate system. The origin of this coordinate system is located at I; positive X readings are to the left in the direction of T; positive Y readings are upward from I as shown. Appropriate mechanical coordinate data will be referred to this coordinate system. First the electro-optical data for each point which was taken directly (not through the leading edge mirror) was used to compute coordinates as follows:

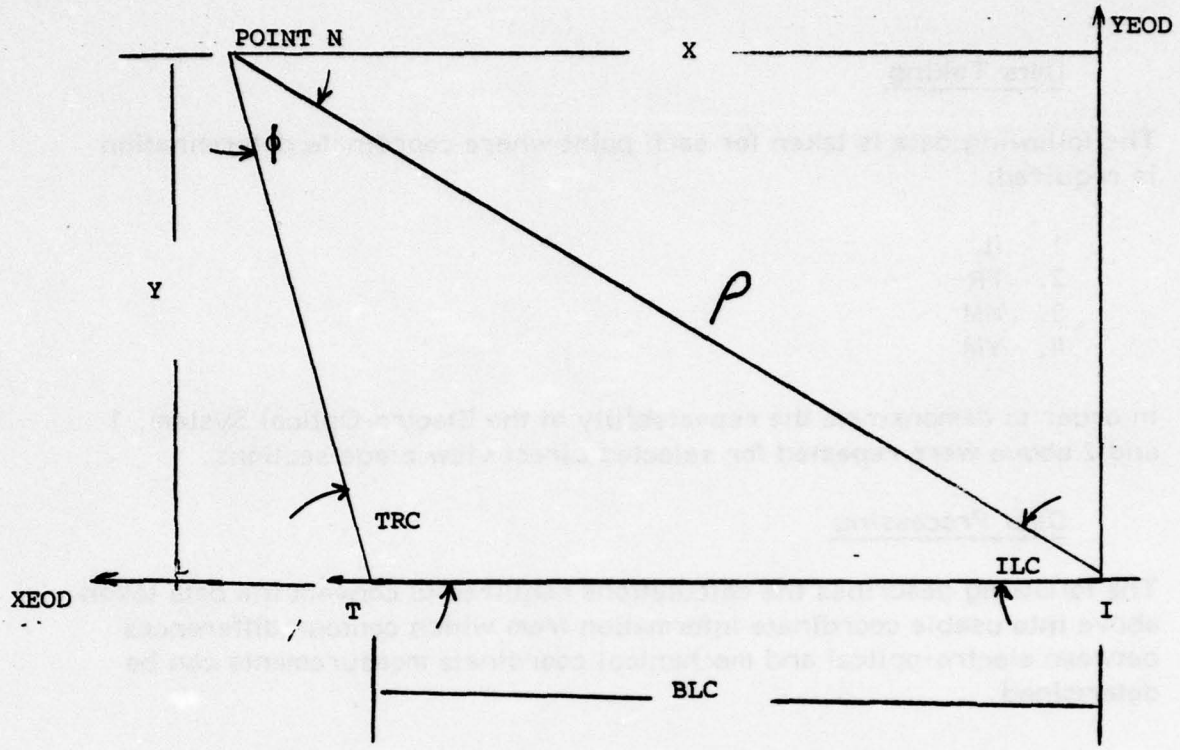

DIRECT VIEW

ELECTRO-OPTICAL
COORDINATE
CALCULATION

FIGURE 9

ILC = IL - IOI

IOI was determined during initial calibration to be - 0.3343°

ILC = IL - 0.3343

TRC = TR - IOT

IOT was determined during initial calibration to be - 0.8247°

TRC = TR - 0.8247°

Calculate actual baseline

This calculation is necessary to account for the fact that the optical axis of the Tracker and Illuminator do not pass through the points of rotation of the Tracker and Illuminator but are eccentric.

BLC = 40 - .0240/sin TRC

The above equation was determined during initial calibration and alignment.

Calculate the coordinate of point N as follows: (See Figure 9)

Law of sines:

$$\frac{\text{Sin TRC}}{\rho} = \frac{\text{Sin } \phi}{\text{BLC}}$$

$$\phi = 180 - \text{ILC} - \text{TRC}$$

$$\rho = \frac{\text{BLC Sin TRC}}{\text{Sin (180-ILC-TRC)}}$$

$$X = \rho \text{ Cos ILC}$$

$$X = \frac{\text{BLC Sin TRC Cos ILC}}{\text{Sin (180-ILC-TRC)}}$$

$$Y = \rho \text{ Sin ILC}$$

$$Y = \frac{\text{BLC Sin TRC Sin ILC}}{\text{Sin (180 - ILC-TRC)}}$$

XEOM and YEOM Calculations

Introduction

The determination of XEOM and YEOM which are the electro-optical coordinates of the leading edge of the rotor section obtained with the aid of the mirror is somewhat more complex than that required for XEOD and YEOD as an iterative process is required when the mirror is used.

Discussion

In order to determine XEOM and YEOM, the exact position of the mirror used in relation to the electro-optical baseline of the system must be determined. This is done by an iterative process; referring to Figure 10, the illuminator optical spindle axis designated I (o,o) serves as the origin of the coordinate system. The tracker optical spindle axis is designated as T (t,o). See Figure 10.

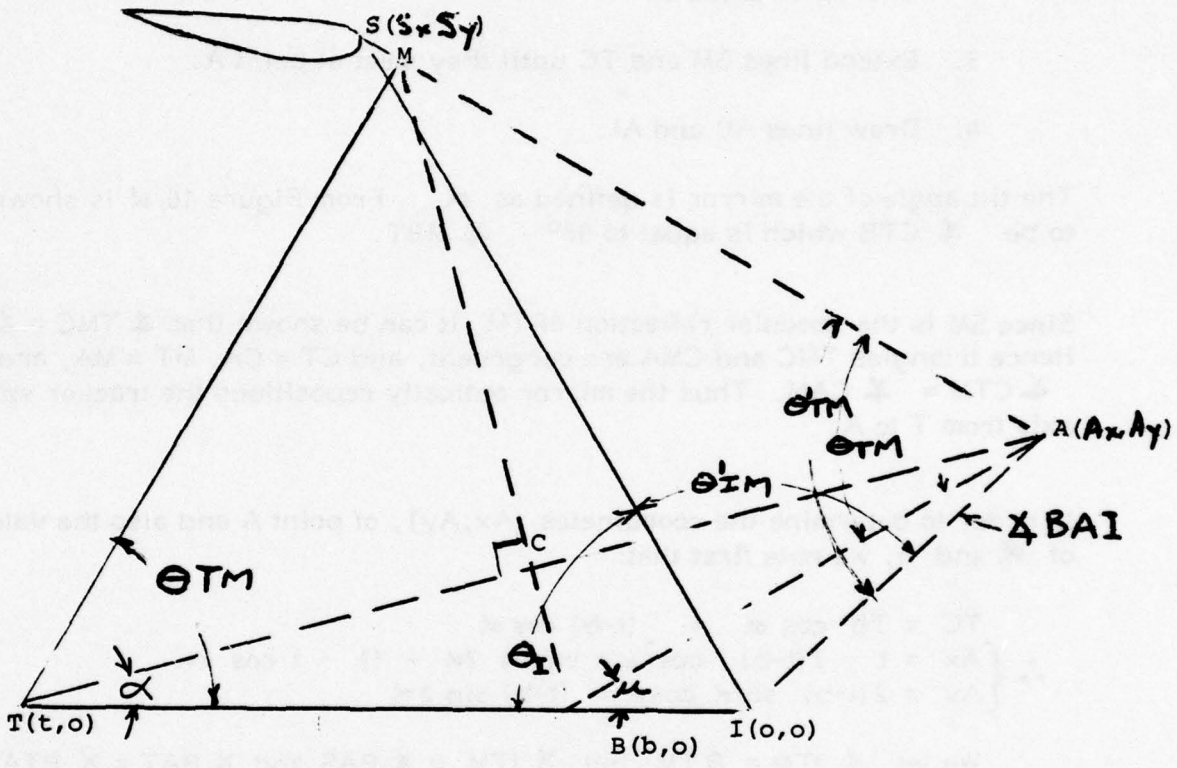

MIRROR VIEW

ELECTRO-OPTICAL
COORDINATE
GEOMETRY

FIGURE 10

S is an illuminated point on the leading edge of the rotor with coordinates (Sx,Sy). M is the point on the mirror surface through which the chief ray of the tracker views S by specular reflection when the tracker is pointed at S.

The following constructions are now made:

1. Extend the line of the mirror surface to meet baseline TI at point B (b,o).

2. Drop a perpendicular from point T to line MB intersecting line MB in point C.

3. Extend lines SM and TC until they meet at point A.

4. Draw lines AB and AI.

The tilt angle of the mirror is defined as α. From Figure 10, α is shown to be $\measuredangle$ CTB which is equal to $90^o - \measuredangle$ MBT.

Since SM is the specular reflection of TM, it can be shown that $\measuredangle$ TMC = $\measuredangle$ CMA. Hence triangles TMC and CMA are congruent, and CT = CA, MT = MA, and $\measuredangle$ CTM = $\measuredangle$ CAM. Thus the mirror optically repositions the tracker spindle axis from T to A.

In order to determine the coordinates (Ax,Ay), of point A and also the values of α and b, we note first that:

$$TC = TB \cos\alpha = (t-b)\cos\alpha$$

$$\therefore \begin{cases} Ax = t - 2(t-b)\cos^2\alpha = b(\cos 2\alpha + 1) - t\cos 2\alpha \\ Ay = 2(t-b)\sin\alpha\cos\alpha = (t-b)\sin 2\alpha \end{cases}$$

We let $\measuredangle$ ITM = θTM; but $\measuredangle$ ITM = $\measuredangle$ BAS, and $\measuredangle$ BAT = $\measuredangle$ BTA = α

$$\frac{Sy-Ay}{Sx-Ax} = \tan(\measuredangle BAS - 2\alpha) = \tan[\theta TM - 2\alpha) \text{ by geometric construction}$$

Substituting in this last equation for Ax and Ay:

$$Sy - (t-b)\sin 2\alpha = \tan(\theta TM - 2\alpha)\left[Sx + (t-b)\cos 2\alpha - b\right]$$

Letting $2\alpha = u$, and $(t-b) = v$, we get:

$$Sy - v\sin u = \tan(\theta TM - u)\left[Sx + v(\cos u + 1) - t\right]$$

$$Sy + (t-Sx)\tan(\theta TM - u) = v\left[(\cos u + 1)\tan(\theta TM - u) + \sin u\right]$$

$$\therefore v = \frac{Sy + (t-Sx)\tan(\theta TM - u)}{\sin u + (1+\cos u)\tan(\theta TM - u)}$$

Procedure

1. Using a point that can be viewed both directly and through the mirror calculate the coordinates by direct view method.

2. With Illuminator stationary rotate Tracker to see the same point in mirror as in (1) above.

3. Record Tracker angle minus 0.8247^{o}; call this corrected Tracker angle ΘTM or ITM (see Figure 10).

4. Determine intersection of Tracker optical axis with 40" baseline. Intersection is at point t where $t = 40 - .024/\sin \Theta TM$.

5. Assume a value for α based upon physical geometry of set up. Call $u = 2\alpha$.

6. Calculate v where $v = \dfrac{Sy + (t-Sx) \tan (\Theta TM - u)}{\sin u + (1 + \cos u) \tan (\Theta TM - u)}$

7. By definition $b = t - v$.

8. We now know b for an assumed value of α .

9. Repeat 1 through 8 above for another point using same assumed α value.

10. Now by iteration repeat 1 through 9 above using different assumed α value until the value of b is same for both points.

11. We now know b and α .

12. Calculations.

12.1

For the (Sx,Sy) point which is the nearer one to the leading edge of the two points used in 8 and 9 above to determine α and b, now calculate:

a) $\alpha = u / 2$

b) $b = t-v$

c) $Ay = AB \sin u = v \sin u$

d) $Ax = -AB \cos u + b = - v \cos u + b$

e) $AI = (Ax^2 + Ay^2)^{1/2}$

f) $\measuredangle BAI = \sin^{-1} \left[\dfrac{b \sin u}{AI}\right]$

g) $\measuredangle BIA = 180^{o} - \measuredangle BAI - 2\alpha$

h) $\Theta' IM = \measuredangle BIA - \Theta I$

i) $\Theta' TM = \measuredangle BAI + \Theta TM$

12.2

IA' values to be applied to the equations of subpara 13 represent the line AI in Figure 10 and may be calculated using equations a) through e) of subpara 12.1 with α and b having the same constant values already determined but with the t value changing for other N points according to the relation of step 4 on the previous page.

Alternatively, applying the law of cosines to triangle ATI of Figure 10, we have:

$$AI = \sqrt{t^2 + [4(t-b)^2 - 4t(t-b)]\cos^2\alpha}$$

In order to devise a simplified formula for calculating the small changes in AI to be used in contouring various points along the leading edge, a first approximation is introduced by treating the last term under the radical as if it were $\cos\alpha$ instead of $\cos^2\alpha$. Thus, the expression under the radical becomes a perfect square and AI is approximately equal to $t - 2(t-b)\cos\alpha$. Now, letting subscript o refer to data pertaining to the point nearer to the leading edge and subscript 1 to data of any other point reflected on the fixed position mirror and reidentifying the line AI as the approximate quantity IA_1, we proceed as follows:

$$IA_1 = IAo + t_1 - 2(t-b)\cos\alpha - to + 2(to - b)\cos\alpha$$

which reduces to

$$IA_1 = IAo + (t_1 - to)(1-2\cos\alpha)$$

A second approximation is introduced at this point by letting $\cos\alpha = 1$ which results in a small error if α is less than 11.5^o or $\cos\alpha \geq .98$. Thus, $IA_1 = IAo + to - t_1$.

Recalling that $t = 40 - .024 \csc \Theta TM$, we have:

$$IA_1 = IAo - .024 \csc \Theta TMo + .024 \csc \Theta TM_1,$$

where this IA_1 is the IA' value applied to the equations of subpara 13 for the determination of XEOM, YEOM coordinates of point N.

13. Using the data obtained in 12.2 and 12.1 above calculate the coordinates of all points as follows (See Figure 11):

Law of sines:

$$\frac{\text{Sin } \Theta'TM}{\rho} = \frac{\text{Sin } \phi}{IA'}$$

$$\phi = 180 - \Theta'IM - \Theta'TM$$

$$\rho = \frac{IA' \text{ Sin } \Theta'TM}{\text{Sin } (180 - \Theta'IM - \Theta'TM)}$$

$$X = \rho \text{ Cos } \Theta'IM$$

$$X = \frac{IA' \text{ Sin } \Theta'TM \text{ Cos } \Theta'IM}{\text{Sin } (180 - \Theta'IM - \Theta'TM)}$$

$$Y = \text{Sin } \Theta'IM$$

$$Y = \frac{IA' \text{ Sin } \Theta'TM \text{ Sin } \Theta'IM}{\text{Sin } (180 - \Theta'IM - \Theta'TM)}$$

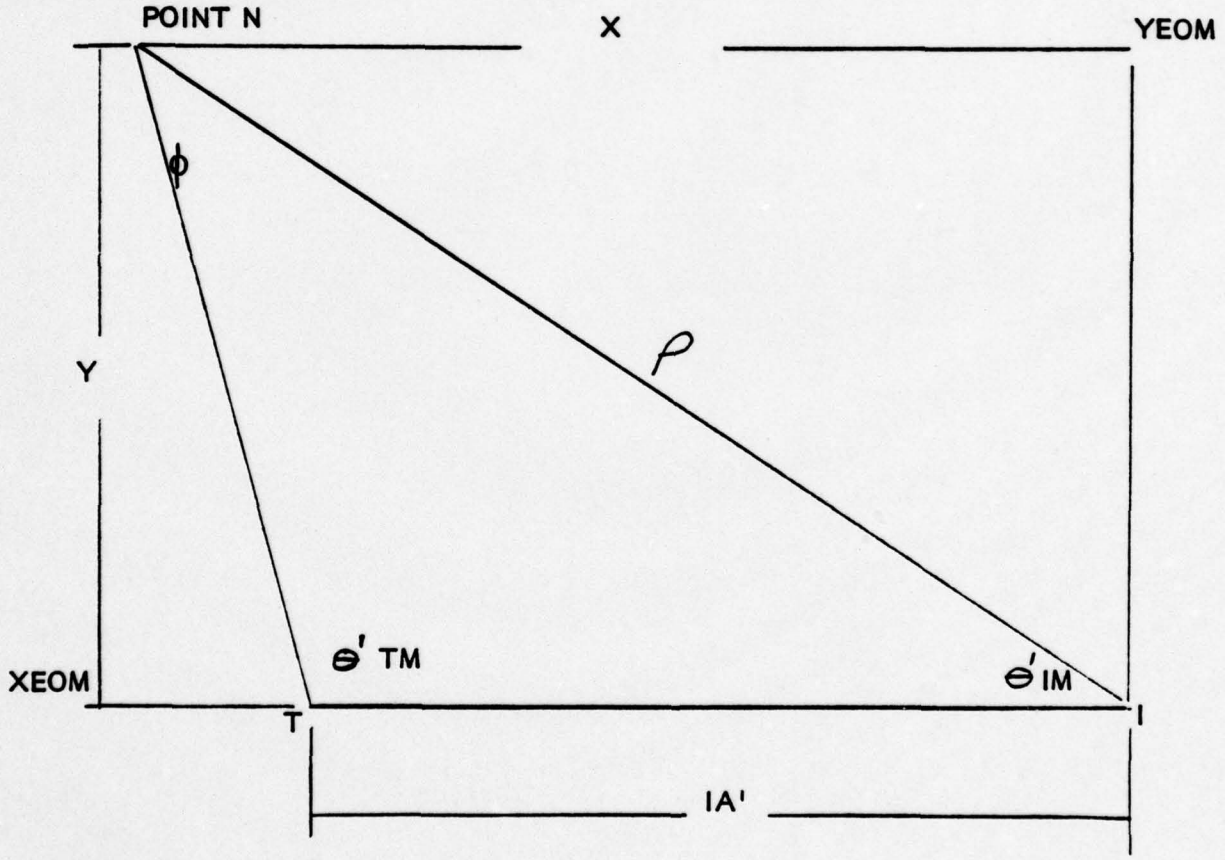

MIRROR VIEW

ELECTRO-OPTICAL
COORDINATE
CALCULATION

FIGURE 11

Rotation of Mechanical Coordinates

Rotation of the mechanical coordinates is accomplished by rotating a point other than the one previously translated about the point previously translated so that the YMT coordinate is equal to YEOD. All other mechanical points are rotated a like amount. See Figure 12 for direct view coordinates and Figure 13 for mirror view coordinates.

Probe Shape Correction

The probe of the dial indicator used to make the YM measurements that are being compared to the YEOD measurements has a 1/16" DIA ball tip. Due to the slope of the rotor section being measured, Y errors will result if a correction is not made. Note: This correction does not apply to the mechanical measurements made that correspond to electro-optical measurements made using the mirror for leading edge readings of the Bell 214-015-001, Bell 654-015-001-1 and Hughes AAH Sections. A conical tip probe was used for these readings and although small errors result from the use of this probe, they are not corrected.

$$YMC = YM - \left(\frac{.031}{\cos\alpha} - .031\right)$$

$$\alpha = \text{Arc tan } \frac{YM \text{ point } N - YM \text{ point } (N+1)}{XM \text{ point } N - XM \text{ point } (N+1)}$$ where N and N+1 are two successive adjacent points

Translation of Mechanical Coordinates

Translate the mechanical measurements of the points whose electro-optical coordinate were determined in 6.1 and 6.2 above to the electro-optical coordinate system (See Figure 7). This transformation is done by taking one common point on the rotor and translating the mechanical coordinates of this point in X and Y so that they are identical to the same point's electro-optical coordinates. Then translate all other mechanical points by a like amount as follows:

For Translation of Points Associates with Direct View

(a) $XMT = XM + A$ where $A = XEOD - XM$ (of the common point)
(b) $YMCT = -YMC + B$ where $B = YEOD + YM$ (of the common point)

A represents the translated distance between the YM axis of Figure 8 and parallel YMCT axis (not shown) which passes through the origin of the XEOD, YEOD coordinate system. Similarly, B represents the translated distance between the XM axis and a parallel XMT axis through the origin of the XEOD, YEOD coordinate system. Values for A and B as they apply to the points N of the tabulated data may be derived using equations (a) and (b) above.

For Translation of Points Associated with Mirror View

$$XMT = XM + A$$
$$YMT = -YM + B$$

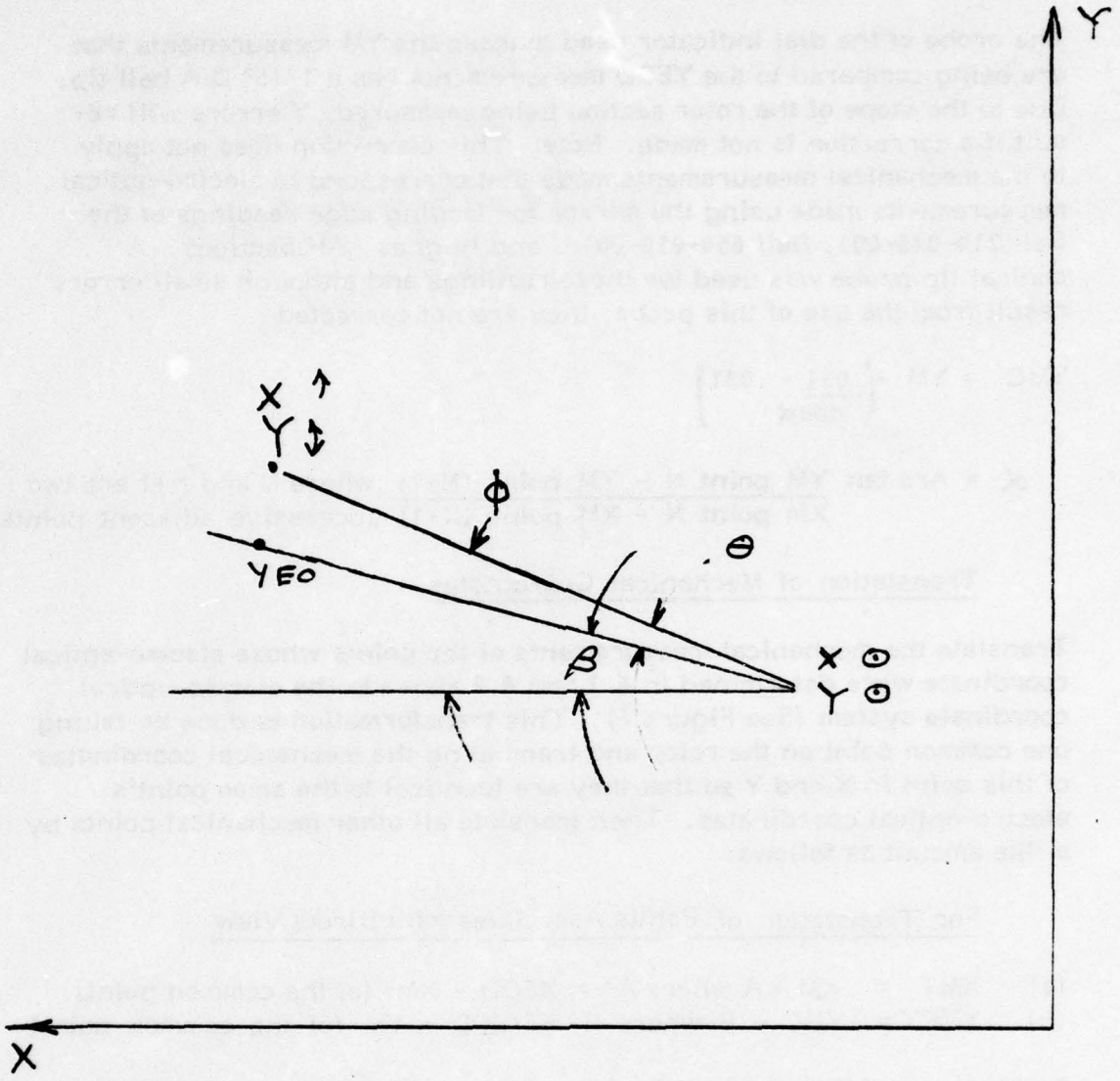

Note: θ is positive for clockwise rotation as shown.

DIRECT VIEW

ROTATION
GEOMETRY

FIGURE 12

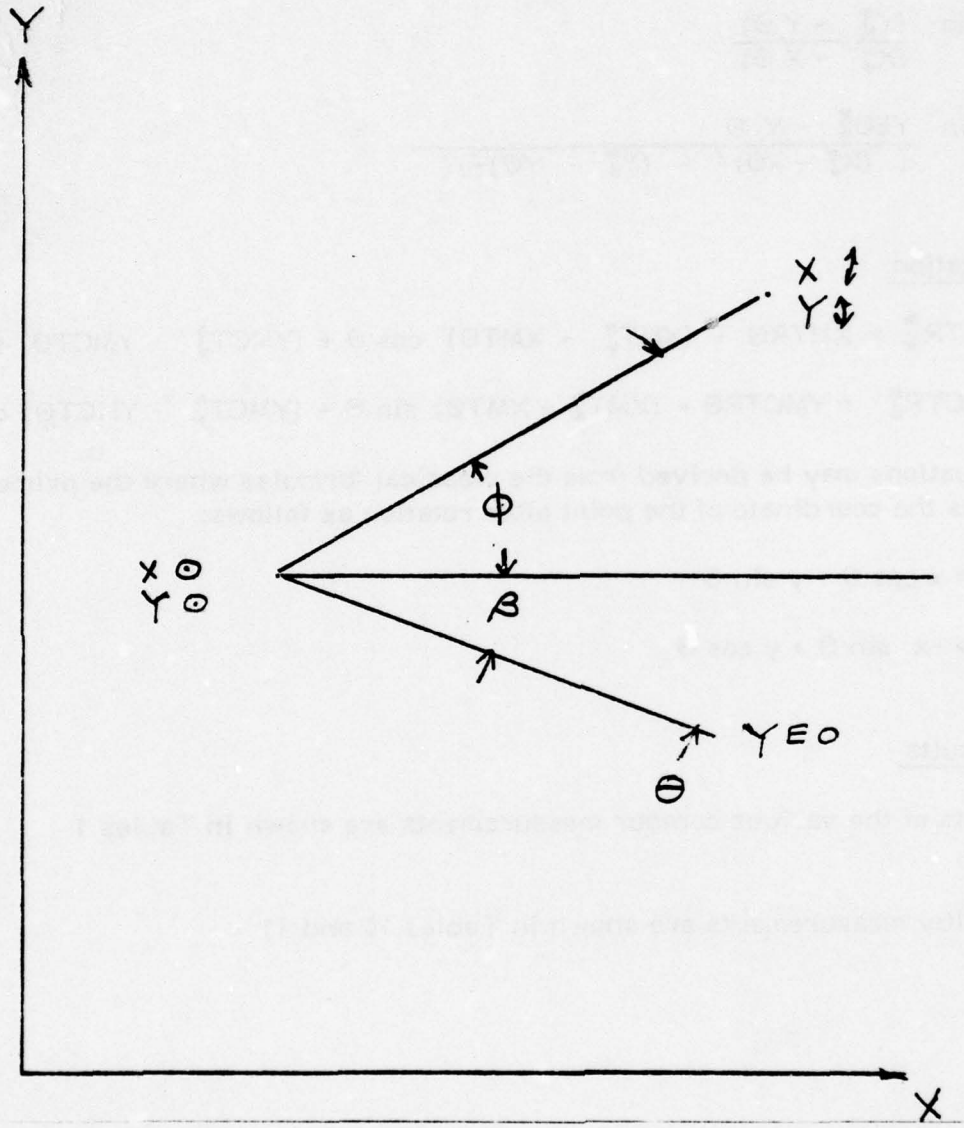

Note: θ is positive for counterclockwise rotation as shown.

MIRROR VIEW

ROTATION
GEOMETRY

FIGURE 13

Angle of Rotation Determination

$\Theta = \phi - \beta$ sign as noted on Figures 12 & 13

$$\phi = \arctan \frac{(Y\updownarrow - Y\odot)}{(X\updownarrow - X\odot)}$$

$$\beta = \arcsin \frac{YEO\updownarrow - Y\odot}{((X\updownarrow - x\odot)^2 + (Y\updownarrow - Y\odot)^2)^{\frac{1}{2}}}$$

Rotation

(a) $XMTR\updownarrow = XMTR\odot + (XMT\updownarrow - XMT\odot)\cos\Theta + (YMCT\updownarrow - YMCT\odot)\sin\Theta$

(b) $YMCTR\updownarrow = YMCTR\odot - (XMT\updownarrow - XMT\odot)\sin\Theta + (YMCT\updownarrow - YMCT\odot)\cos\Theta$

These equations may be derived from the classical formulas where the prime represents the coordinate of the point after rotation as follows:

(c) $x' = x\cos\Theta + y\sin\Theta$

(d) $y' = -x\sin\Theta + y\cos\Theta$

Results

The results of the various contour measurements are shown in Tables 1 through 9.

Repeatability measurements are shown in Tables 10 and 11.

TABLE 1
ROTOR BLADE MEASUREMENT DATA
DIRECT VIEW
ROTOR SECTION BELL 214-015-001 PAINTED SURFACE

N	82.53	74.91	67.30	59.71	53.80	48.73	43.65	37.04	29.47	21.90	16.85	11.77	8.18	5.10
IL	34.4049	35.6692	37.0098	38.5500	39.8811	41.1223	42.4754	44.7300	47.2669	50.1312	52.2889	54.7015	56.5632	58.2706
TR	109.2350	104.8812	100.2661	95.3642	91.4024	87.9521	84.4706	79.2770	74.2309	69.4429	66.4585	63.7062	62.0046	60.7486
XM	15.6350	12.6350	9.6350	6.6350	22.0930	20.0930	18.0930	15.0870	12.0850	9.0930	7.0930	5.0930	3.7100	2.5465
YM	.1071	.3582	.6581	.8820	.1735	.3830	.5649	.7849	.9481	1.0270	.9789	.7910	.5129	.1367
BLC	39.9747	39.9753	39.9757	39.9759	39.9760	39.9760	39.9759	39.9755	39.9751	39.9742	39.9737	39.9730	39.9726	39.9723
XEOD	51.5877	48.6022	45.6263	42.6409	40.3116	38.3170	36.3164	33.3113	30.3111	27.3187	25.3201	23.3149	21.9290	20.7698
YEOD	34.8882	34.4564	33.9786	33.5746	33.2865	33.0610	32.8617	32.6155	32.4286	32.3238	32.3548	32.5268	32.7936	33.1574
α	4.8	5.7	4.3	3.6	6.0	5.2	4.2	3.1	1.5	0	5.4	11.4	17.9	22.4
YMC	.1070	.3580	.6580	.8819	.1733	.3829	.5648	.7849	.9481	1.0270	.9788	.7904	.5113	.1342
XMT	51.6409	48.6409	45.6409	42.6409	40.3120	38.3120	36.3120	33.3060	30.3040	27.3120	25.3120	23.3120	21.929	20.7655
YMCT	34.3495	34.0985	33.7985	33.5746	33.1317	32.9220	32.7401	32.5200	32.3568	32.2779	32.3261	32.5145	32.7936	33.1707
XMTR	51.5782	48.5986	45.6221	42.6409	40.3085	38.3103	36.3119	33.3079	30.3074	27.3162	25.3158	23.3143	21.9290	20.7624
YMTR	34.8882	34.4576	33.9781	33.5746	33.2865	33.0600	32.8612	32.6158	32.4273	32.3233	32.3546	32.5262	32.7936	33.1609
XE	-.0095	-.0036	-.0042	0	-.0031	-.0067	-.0045	-.0034	-.0037	-.0025	-.0043	-.0006	0	-.0074
YE	0	.0012	-.0005	0	0	.0010	-.0005	.0003	.0013	-.0005	-.0002	-.0006	0	.0035

TABLE 2
ROTOR BLADE MEASUREMENT DATA
MIRROR VIEW
ROTOR SECTION BELL 214-015-001 PAINTED

N	8.15	5.09	2.10	1.77	1.42	1.07	0.71	0.53	0.33	0.10	0.02	0.00	-0.03
IL	55.4998	57.2498	59.0001	59.1999	59.3998	59.5997	59.8000	59.8999	59.9996	60.0995	60.1300	60.1403	60.1495
TR	51.0651	52.1504	53.3931	53.5527	53.7167	55.8876	54.0689	54.1643	54.2664	54.3840	54.4265	54.4412	54.4551
XM	7.0605	5.8628	4.6815	4.5605	4.4195	4.2900	4.1485	4.0905	4.0200	3.9540	3.9325	3.9275	3.9205
YM	.4703	.6825	.7109	.6960	.6710	.6399	.5923	.5668	.5278	.4717	.4460	.4373	.4273
BLC	23.3083	23.3088	23.3093	23.3094	23.3094	23.3095	23.3096	23.3096	23.3096	23.3097	23.3097	23.3097	23.3097
XEOM	1.1539	2.3149	3.4751	3.6093	3.7441	3.8799	4.0176	4.0871	4.1575	4.2305	4.2538	4.2617	4.2689
YEOM	38.6497	38.2881	38.1109	38.1122	38.1184	38.1335	38.1615	38.1818	38.2113	38.2617	38.2861	38.2947	38.3036
XMT	1.1539	2.3516	3.5329	3.6539	3.7949	3.9244	4.0659	4.1239	4.1944	4.2604	4.2819	4.2869	4.2939
YMT	38.6497	38.4375	38.4091	38.4240	38.4490	38.4801	38.5277	38.5532	38.5922	38.6483	38.6740	38.6827	38.6927
XMTR	1.1539	2.3155	3.4839	3.6058	3.7489	3.8812	4.0276	4.0883	4.1632	4.2357	4.2608	4.2663	4.2745
YMCTR	38.6497	38.2890	38.1126	38.1122	38.1193	38.1339	38.1634	38.1815	38.2113	38.2587	38.2815	38.2894	38.2985
XE	0	.0006	.0088	-.0035	.0048	.0013	.0100	.0012	.0057	-.0052	-.0064	.0046	.0056
YE	0	.0009	.0017	0	.0009	.0004	.0019	.0005	0	-.0030	-.0046	-.0053	-.0051

TABLE 3
ROTOR BLADE MEASUREMENT DATA
DIRECT VIEW
ROTOR SECTION BELL 654-015-001-1 PAINTED

N	24.65	22.82	20.47	17.60	14.60	11.08	8.34	6.17	3.87	1.58
IL	50.3009	50.9716	51.7564	52.7415	53.8392	55.2729	56.4895	57.5413	58.7381	60.0120
TR	73.0480	71.9400	70.4895	68.7527	66.9621	64.9447	63.4529	62.3477	61.2904	60.4215
XM	10.7292	10.0107	9.0898	7.9770	6.8067	5.4257	4.3460	3.4883	2.5932	1.7460
YM	.2020	.2445	.4060	.5981	.7807	.9006	.9233	.8708	.7172	.4205
BLC	39.9748	39.9746	39.9744	39.3941	39.9738	39.9733	39.9730	39.9727	39.9724	39.9721
XEOD	28.9329	28.2107	27.2934	26.1838	25.0160	23.6347	22.5569	21.7012	20.8069	19.9533
YEOD	34.4393	34.3891	34.2162	34.0087	33.8132	33.6773	33.6388	33.6835	33.8270	34.1161
α	4.0	10.7	10.[illegible]	9.5	5.6	2.0	3.0	9.1	12.4	12.4
YMC	.2019	.2440	.4055	.5977	.7806	.9006	.9233	.8705	.7165	.4196
XMT	28.9421	28.2236	27.3027	26.1899	25.0196	23.6386	22.5589	21.7012	20.8061	19.9589
YMCT	34.3521	34.3100	34.1485	33.9563	33.7734	33.6534	33.6307	33.6835	33.8375	34.1344
XMTR	28.9335	28.2156	27.2967	26.1863	25.0183	23.6388	22.5595	21.7012	20.8043	19.9536
YMCTR	34.4393	34.3885	34.2160	34.0104	33.8134	33.6767	33.6410	33.6835	33.8267	34.1134
XE	.0006	.0049	.0033	.0025	.0023	.0041	.0026	0	-.0025	.0003
YE	0	-.0006	-.0002	.0017	.0002	-.0006	.0022	0	-.0003	-.0027

TABLE 4
ROTOR BLADE MEASUREMENT DATA
MIRROR VIEW
ROTOR SECTION BELL 654-015-001-1 PAINTED

N	6.17	3.87	1.58	1.07	0.56	0.07	0
IL	56.8998	58.0998	59.3996	59.7000	60.0001	60.2633	62.2850
TR	52.2273	52.8454	53.6458	53.8571	54.0892	54.3436	54.3735
XM	11.822	10.983	10.101	9.899	9.693	9.517	9.508
YM	2.429	2.731	2.892	2.895	2.873	2.782	2.763
BLC	23.3183	23.3186	23.3189	23.3190	23.3191	23.3192	23.3192
XEOM	2.1329	2.9139	3.7585	3.9556	4.1558	4.3383	4.3548
YEOM	38.7670	38.3148	37.9994	37.9599	37.9475	38.0039	38.0205
XMT	2.1329	2.9719	3.8539	4.0559	4.2619	4.4379	4.4469
YMT	38.767	38.465	38.304	38.301	38.325	38.414	38.433
XMTR	2.1329	2.9035	3.7419	3.9400	4.1470	4.3361	4.3484
YMTR	38.7670	38.3183	38.0006	37.9611	37.9475	38.0032	38.0203
XE	0	-.0104	-.0166	-.0156	-.0088	-.0022	-.0100
YE	0	.0035	.0012	.0012	0	.0007	.0002

TABLE 5
ROTOR BLADE MEASUREMENT DATA
DIRECT VIEW
ROTOR SECTION HUGHES AAH PAINTED

N	54.01	52.48	49.95	42.24	34.53	26.87	19.28	11.67	7.74	4.50	1.48
IL	40.3975	40.8585	41.6431	43.4895	45.5241	47.9632	50.8388	54.2292	56.1919	57.9473	59.6906
TR	90.8784	89.8544	88.1557	82.9771	77.7594	72.6664	67.8719	63.5037	61.4851	60.0196	58.9627
XM	23.4020	22.8020	21.7960	18.796	15.8020	12.8020	9.8020	6.7990	5.2480	3.9980	2.8970
YM	.4107	.3758	.3162	.8856	1.4676	1.8670	2.0748	2.0420	1.8979	1.6480	1.2100
BLC	39.9760	39.9760	39.9760	39.9758	39.9754	39.9747	39.9739	39.9730	39.9727	39.9721	39.9717
XEOD	40.0075	39.4055	38,4029	35.4011	32.4050	29.4028	26.4062	23.3992	21.8563	20.6039	19.5065
YEOD	33.6464	33.6850	33.7487	33.1912	32.6201	32.2329	32.0376	32.0824	32.2308	32.4837	32.9271
α	3.3	3.4	3.4	11.1	7.6	4.0	.6	5.3	13.1	13.9	33.2
YMC	.4106	.3757	.3166	.8885	1.4673	1.8669	2.0748	2.0419	1.8971	1.6471	1.2040
XMT	40.0022	39.4022	38.3962	35.3962	32.4022	29.4022	26.4022	23.3992	21.8482	20.5982	19.4972
YMCT	33.7137	33.7486	33.8077	33.2358	32.6570	32.2574	32.0495	32.0824	32.2272	32.4772	32.9203
XMTR	40.0087	39.4088	38.4031	35.4008	32.4045	29.4029	26.4020	23.3992	21.8488	20.5998	19.5006
YMCTR	33.6464	33.6837	33.7469	33.1872	32.6205	32.2331	32.0373	32.0824	32.2372	32.4885	32.9361
XE	.0012	.0033	.0002	-.0003	-.0005	.0001	-.0042	0	-.0075	-.0041	-.0059
YE	0	-.0013	-.0018	-.0040	-.0004	-.0008	-.0003	0	.0027	.0048	-.0068

TABLE 6
ROTOR BLADE MEASUREMENT DATA
MIRROR VIEW
ROTOR SECTION HUGHES AAH PAINTED

N	7.74	4.50	1.48	0.60	0.15	0
IL	55.5001	57.2500	59.0001	59.5095	59.7480	59.8066
TR	51.1256	52.0908	53.2443	53.6587	53.8955	53.9664
XM	11.5330	10.2910	9.1190	8.7840	8.6400	8.6080
YM	2.1880	2.5030	2.5770	2.4970	2.4070	2.3820
BLC	23.3349	23.3353	23.3358	23.3360	23.3361	23.3361
XEOM	1.1965	2.3484	3.4940	3.8353	4.0013	4.0440
YEOM	38.7123	38.1769	37.8805	37.8936	37.9560	37.9884
XMT	1.1965	2.4385	3.6105	3.9455	4.0895	4.1215
YMT	38.7123	38.3973	38.3233	38.4033	38.4933	38.5183
XMTR	1.1965	2.3581	3.4958	3.8398	3.9981	4.0342
YMTR	38.7123	38.1715	37.8805	37.8967	37.9584	37.9769
XE	0	.0097	.0018	.0045	-.0032	-.0098
YE	0	-.0054	0	.0031	.0024	-.0115

TABLE 7
ROTOR BLADE MEASUREMENT DATA
MIRROR VIEW
ROTOR SECTION KAMAN COBRA-RUBBER

N	7.52	4.98	2.53	1.59	1.08	.56	.15	0
IL	56.0000	57.4000	58.8000	59.3500	59.6500	59.9400	60.1426	60.1950
TR	51.4273	52.2955	53.2444	53.6515	53.8918	54.1489	54.3592	54.4264
XM	7.6890	6.7050	5.7420	5.3721	5.1707	4.9747	4.8430	4.8095
YM	.3228	.5186	.6126	.6054	.5772	.5141	.4218	.3806
BLC	21.7271	21.7275	21.7279	21.7281	21.7282	21.7283	21.7284	21.7284
XEOM	.2331	1.1764	2.1104	2.4777	2.6795	2.8774	3.0194	3.0576
YEOM	39.0169	38.6806	38.4468	38.3989	38.3976	38.4311	38.4986	38.5347
α	15.5	10.5	4.5	3.5	10.5	15.5	44.5	63.5
YMC	.3216	.5181	.6125	.6053	.5770	.5129	.4093	.3421
XMT	.2331	1.2171	2.1801	2.5500	2.7514	2.9474	3.0791	3.1126
YMCT	39.0169	38.8205	38.7260	38.7332	38.7615	38.8256	38.9292	38.9964
XMTR	.2331	1.1782	2.1174	2.4844	2.6878	2.8910	3.0363	3.0792
YMCTR	39.0169	38.6799	38.4468	38.4003	38.3991	38.4341	38.5175	38.5792
XE	0	-.0018	.0070	.0067	.0083	.0136	.0169	.0216
YE	0	-.0007	0	.0014	.0015	.0030	.0189	.0445

TABLE 8
ROTOR BLADE MEASUREMENT DATA
DIRECT VIEW
ROTOR SECTION KAMAN COBRA-UNPAINTED

N	76.35	73.04	68.01	60.19	52.97	45.01	37.79	30.27	25.15	20.10	15.29
IL	34.2000	34.9000	35.8500	37.4750	39.0800	41.0660	43.1000	45.5700	47.5000	49.6000	51.8000
TR	105.9012	103.7514	100.4989	95.2225	90.1813	84.4910	79.3461	74.1430	70.7615	67.6031	64.8008
XM	23.2867	21.9847	20.0058	16.9388	16.5622	13.4127	10.5710	7.6028	5.5870	3.6032	1.7095
YM	-.0001	.0090	.2070	.5070	.5943	.7368	.8254	.7862	.6587	.4608	.1854
BLC	39.9751	39.9754	39.9759	39.9759	39.9760	39.9759	39.9755	39.9749	39.9744	39.9739	39.9733
XEOD	48.7966	47.4846	45.5130	42.4469	39.6189	36.4878	33.6546	30.6994	28.6774	26.6816	24.7815
YEOD	32.7469	32.7150	32.4827	32.1290	31.7933	31.4202	31.1267	30.9528	30.9320	30.9820	31.1157
α	1.2	.8	3.8	4.8	1.6	1.6	.4	2.4	5.4	8.4	11.4
YMC	-.0001	.0090	.2069	.5069	.5943	.7368	.8254	.7862	.6586	.4606	.1848
XMT	48.7948	47.4928	45.5139	42.4469	39.6406	36.4911	33.6494	30.6812	28.6654	26.6816	24.7879
YMCT	32.6358	32.6269	32.4290	32.1290	30.8483	30.7058	30.6172	30.6564	30.7840	30.9820	31.2578
XMTR	48.7850	47.4833	45.5082	42.4469	39.6159	36.4851	33.6575	30.6943	28.6746	26.6816	24.7728
YMCTR	32.7469	32.7152	32.4826	32.1290	31.7933	31.4216	31.1261	30.9488	30.9291	30.9820	31.1190
XE	-.0116	-.0013	-.0048	0	-.0030	-.0027	-.0029	-.0051	-.0028	0	-.0087
YE	0	.0002	.0001	0	0	.0014	-.0006	-.0040	.0029	0	.0033

TABLE 9
ROTOR BLADE MEASUREMENT DATA
DIRECT VIEW
ROTOR SECTION KAMAN COBRA-PAINTED

N	76.00	75.08	74.16	72.77	60.07	52.71	45.20	37.57	30.06	25.06	20.04	15.01	10.09	7.52	4.98
IL	34.3000	34.5000	34.7000	35.0000	37.6000	39.3000	41.2000	43.4000	45.9000	47.8000	49.9000	52.2000	54.6500	56.0000	57.4000
TR	106.1433	105.5447	104.9505	104.0549	95.6600	90.5532	85.2730	79.8579	74.7228	71.4723	68.3562	65.4754	62.9147	61.6791	60.5838
XM	22.9965	22.6300	22.2675	21.7220	16.6960	13.7895	17.5250	14.5060	11.5450	9.5730	7.5760	5.5860	3.6520	2.6520	1.6785
YM	0.1471	0.1351	0.1220	0.1090	0.4253	0.6148	0.3297	0.6939	0.9218	0.9733	0.9625	0.8526	0.6304	0.4777	0.2484
BLC	39.9751	39.9752	39.9753	39.9753	39.9759	39.9760	39.9759	39.9756	39.9750	39.9746	39.9740	39.9734	39.9728	39.9725	39.9722
XEOD	49.0203	48.6501	48.2849	47.7368	42.7257	39.8233	36.8745	33.8455	30.8820	28.9076	26.9125	24.9299	23.0049	22.0061	21.0382
YEOD	33.0213	33.0194	33.0184	33.0118	32.5082	32.2096	31.9036	31.6336	31.4983	31.5095	31.5831	31.7546	32.0334	32.2189	32.4783
α	2.5	2.5	2.5	.4	3.5	3.5	7.3	5.3	3.3	0.3	2.7	5.7	7.7	9.7	14.7
YMC	0.1471	0.1351	0.1220	0.1090	0.4252	0.6147	0.3294	0.6938	0.9217	0.9733	0.9625	0.8524	0.6301	0.4773	0.2474
XMT	49.0303	48.6638	48.3013	47.7558	42.7298	39.8233	36.8689	33.8499	30.8889	28.9169	26.9199	24.9299	22.9959	21.9959	21.0224
YMCT	32.6772	32.6892	32.7023	32.7153	32.3991	32.2096	32.2776	31.9132	31.6853	31.6337	31.6445	31.7546	31.9769	32.1297	32.3596
XMTR	49.0064	48.6397	48.2770	47.7313	42.7207	39.8233	36.8803	33.8505	30.8838	28.9112	26.9155	24.9299	23.0038	22.0091	21.0433
YMCTR	33.0211	33.0194	33.0189	33.0115	32.5076	32.2096	31.9036	31.6339	31.4988	31.5089	31.5823	31.7546	32.0373	32.2214	32.4816
XE	-.0139	-.0104	-.0079	-.0055	-.0050	0	.0058	.0050	.0018	.0036	.003	0	-.0011	.0030	.0050
YE	-.0002	0	-.0005	-.0003	-.0006	0	0	.0003	.0005	-.0006	-.0008	0	.0039	.0025	.0033

TABLE 10
REPEATABILITY MEASUREMENTS
ROTOR SECTION BELL 214-015-001 PAINTED

IL			TR		
Run 1	Run 2	Delta	Run 1	Run 2	Delta
41.1223	41.1223	0	87.9506	87.9508	+.0002
39.8811	39.8811	0	91.4015	91.4013	-.0002
38.5500	38.5500	0	95.3642	95.3643	+.0001
37.0098	37.0098	0	100.2661	100.2659	-.0002
35.6692	35.6692	0	104.8817	104.8816	-.0001
34.4049	34.4049	0	109.2350	109.2349	-.0001

Note: A delta of .0002° amounts to less than 0.0001" change in contour.

TABLE 11
REPEATABILITY MEASUREMENTS
ROTOR SECTION BELL 654-015-001-1 PAINTED

IL			TR		
Run 1	Run 2	Delta	Run 1	Run 2	Delta
60.0120	60.0120	0	60.4215	60.4216	+.0001
58.7381	58.7381	0	61.2904	61.2904	0
57.5413	57.5413	0	62.3477	62.3477	0
56.4895	56.4895	0	63.4529	63.4527	-.0002
55.2729	55.2729	0	64.9447	64.9444	-.0003
53.8392	53.8392	0	66.9621	66.9619	-.0002
52.7415	52.7415	0	68.7527	68.7526	-.0001
51.7564	51.7564	0	70.4895	70.4892	-.0003
50.9716	50.9716	0	71.9400	71.9398	-.0002
50.3009	50.3009	0	73.0480	73.0480	0

Note: A delta of .0003° amounts to approximately 0.0001" change in contour.

Material Reflected Signal Measurements

Samples of rotor blade material were placed on a rotatable pedestal in locations approximating the leading edge, trailing edge and midpoint of a rotor blade. (Figure 14.)

These samples were illuminated and the illuminated spot was captured by the tracker. The signal level of the tracker output was read. The sample was then rotated about the point of illumination until a usable signal was no longer available.

At all three locations on the rotor surface, we found that the sample materials had to be rotated until their surfaces were practically tangent to either the illuminator axis or the tracker axis to make the signal voltage drop below a usable level. Such extreme testing conditions are not realistic; tangency is not a practical operating orientation because:

a. The illuminator generates a light patch on the rotor surface which is no longer a 0.001" diameter dot. The light patch elongates and spreads out over the surface, compromising the accuracy of location of the measured point and its contour data. We recommend limiting the illumination grazing angle to 10^{o} in order to limit spot enlargement to .001"/Sin 10^{o} = 0.006".

b. The tracker's lens aperture becomes vignetted, reducing its tracking accuracy. The tracker aperture subtends up to 5^{o} as seen from the rotor surface; hence we recommend limiting the tracker grazing angle to 10^{o} to avoid vignetting.

In accordance with the operating limits outlined above, we measured the tracker's signal level at grazing angles of 10^{o} relative to the illuminator and tracker.

The above testing indicates that the electro-optical system is not material-limited in operation relative to the materials tested.

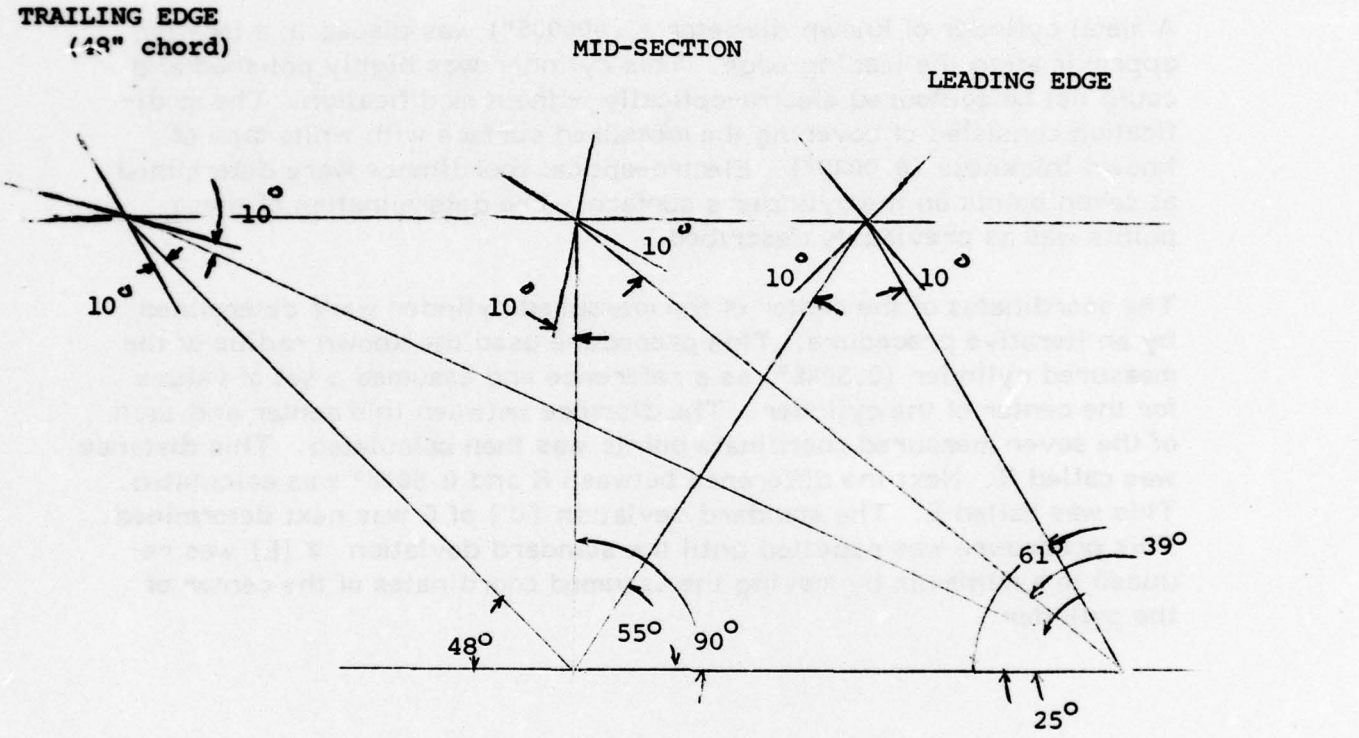

ROTOR REFLECTANCE TEST GEOMETRY

FIGURE 14

Cylinder Contour Measurements

A metal cylinder of known diameter (1.000005") was placed in a location approximating the leading edge. This cylinder was highly polished and could not be contoured electro-optically without modification. The modification consisted of covering the measured surface with white tape of known thickness (0.0048"). Electro-optical coordinates were determined at seven points on the cylinder's surface. The determination of these points was as previously described.

The coordinates of the center of the measured cylinder were determined by an iterative procedure. This procedure used the known radius of the measured cylinder (0.5048") as a reference and assumed a set of values for the center of the cylinder. The distance between this center and each of the seven measured coordinate points was then calculated. This distance was called R. Next the difference between R and 0.5048" was calculated. This was called E. The standard deviation (σ) of E was next determined. This procedure was repeated until the standard deviation σ (E) was reduced to a minimum by moving the assumed coordinates of the center of the cylinder.

10. TEST RESULTS

The purpose of the effort performed under this Phase I contract was to show that the Dreyfus-Pellman concept of non-contact electro-optical contouring of helicopter rotor blades was technically feasible and could be applied to the construction of a computer controlled machine that could measure the contour of helicopter rotor blades in a factory environment to much closer accuracies than currently practical.

Contour Measurement

Prior to signal to noise ratio increase, sixty-one data points were taken; the average difference between electro-optical and mechanical measurements in X (along the chord) was 0.0042" and in Y (chord thickness) was 0.0016". The following table is a summary of differences:

TABLE 12
SUMMARY OF DIFFERENCES
LOW SIGNAL TO NOISE RATIO

Difference Magnitude	Number of Points	
	X	Y
Less than 0.0005"	12	24
Less than 0.0010"	15	35
Less than 0.0015"	18	41
Less than 0.0020"	19	45
Less than 0.0030"	25	49
Less than 0.0040"	34	53
Less than 0.0050"	43	56
Total Points	61	61

Repeatability of results has been demonstrated to be better than 0.0001". The repeatability and accuracy of the electro-optical measurements are an order of magnitude better than the corresponding mechanical measurements. What we call difference is the difference between the electro-optical reading and the mechanical reading; this is not a true error of electro-optical reading. The method of analysis required that the exact same point be measured mechanically and electro-optically. This was done to an accuracy of $\pm$ 0.005". Therefore, this difference in reading is attributed to inaccuracies in mechanical measurement and differences in where the measurements were taken. The portion of differences that can be attributed to the electro-optical system is approximately 10% of the total difference.

The improved signal-to-noise ratio was sufficient to measure the contour of the neoprene rubber nose section of the Cobra blade. Eight points were measured. Due to the resilience of the neoprene rubber it was not possible to get accurate mechanical measurements when the contact angle between the probe and blade exceeded 25°. In cases where this angle was less than 25°, reasonable (to an accuracy of 0.003") mechanical measurements were obtained.

In cases where the contact angle was less than 25°, correspondence between electro-optical measurement and mechanical measurement was as follows:

TABLE 13
SUMMARY OF DIFFERENCES
RUBBER SURFACE; IMPROVED SIGNAL TO NOISE RATIO

Difference Magnitude	Number of Points	
	X	Y
Less than 0.001"	1	3
Less than 0.0015"		4
Less than 0.002"	2	5
Less than 0.003"		
Less than 0.005"		6
Less than 0.010"	5	
Total Points	6	6

Measurements of eleven points on the unpainted fiberglas surface yielded the following results:

TABLE 14
SUMMARY OF DIFFERENCES
IMPROVED SIGNAL-TO-NOISE RATIO UNPAINTED

Difference Magnitude	Number of Points	
	X	Y
Less than 0.001"	2	7
Less than 0.0015"	3	8
Less than 0.002"	3	10
Less than 0.003"	6	10
Less than 0.005"	9	11
Less than 0.010"	10	11
Total Points	11	11

Measurements of fifteen points on the painted surface yielded the following results:

TABLE 15
SUMMARY OF DIFFERENCES
IMPROVED SIGNAL-TO-NOISE RATIO PAINTED

Difference Magnitude	Number of Points	
	X	Y
Less than 0.001"	2	12
Less than 0.0015"	3	
Less than 0.002"	4	
Less than 0.003"		13
Less than 0.005"	7	15
Less than 0.010"	13	
Total Points	15	15

The results of the above test demonstrate that the electro-optical contouring system will give highly accurate results on either painted or unpainted fiberglas and on low-reflecting materials such as black neoprene rubber. Slightly better accuracy was obtained on the painted fiberglas material but the results of these tests indicate that high accuracy contours can be obtained on unpainted surfaces.

The above results demonstrate rather conclusively the viability of the concept and lead us to conclude that the construction of a prototype machine employing these principles is a natural next step.

MATERIAL REFLECTED SIGNAL MEASUREMENTS

The system has a fundamental limit to its measuring speed and contouring accuracy. This fundamental limit is related to certain limits in the system's information rate capacity which can be expressed in digital bit-rate terms. These limits derive from the fact that light flows in tiny lumps called photons. Statistical shot noise in the photon flux limits the speed and accuracy with which we can measure the brightness and location of a light spot.

The system's light source is a helium-neon laser radiating 5 milliwatts at a wavelength of 0.6328 microns. At this wavelength, each photon contains an energy of $(6.6252 \times 10^{-34}$ watt $sec^2)$ $(2.99793 \times 10^{+10}$ cm/sec$)/0.6328 \times 10^{-4}$ cm $= 3.139 \times 10^{-19}$ watt seconds; hence a five milliwatt light beam contains a flow of $5 \times 10^{-3}/3.139 \times 10^{-19} = 1.593 \times 10^{+16}$ photons per second.

The system's optical train contains 14 glass/air surfaces, each with approximately 4% reflection loss; three aluminum mirrors, each with about 80% reflectivity; one light chopper with 50% duty cycle; and one interference filter with about 50% transmittance; hence the optical system has an overall transmissive efficiency of $0.96^{14} \times 0.8^3 \times 0.5^2 = 0.07$.

The system's light detector has a quantum efficiency of about 10%; i.e. it generates one electron for every ten incident photons. The frame rate of the system is 10^3 frames per second; i.e. it receives light reflected from the rotor surface for 10^{-3} seconds while measuring the contour location of each surface point. Hence the system's bit count per frame is $(1.593 \times 10^{+16})$ (0.07) (10^{-1}) $(10^{-3}) = 1 \times 10^{+11}$ electrons/frame, neglecting sample surface attenuation.

In order to determine the location of the illuminated rotor spot within the tracker's field of view, the system measures the difference in electrical output of the detector's left and right quadrant pairs during each frame. The tracker has a field of view of $\pm$ .050" on the rotor surface; the location of the illuminated rotor spot within the tracker's field of view is determined to $\pm$ .0005" accuracy by measuring the quadrant pair output difference to 1% accuracy during each frame. Photometric measurement to 1% accuracy requires a bit count of 10^{+4} electrons per frame because Poisson statistical

shot noise generates an rms noise level equal to the square root of the frame's bit count. Therefore the system's bit rate after sample surface attenuation must be at least 10^{+4} electrons per frame. We note in passing that there are $6.242 \times 10^{+18}$ electrons per second in a current flow of one ampere.

Sample surface attenuation can be estimated by modeling the rotor surface as a planar white Lambertian reflector such as a block of chalk oriented parallel to the baseline. The light diffusely reflected from such a Lambertian reflector fills a 2π steradian hemisphere; of this energy the tracker intercepts 1/200 with its 2" square entrance pupil located at a distance of approximately 30" from the rotor. Hence a Lambertian rotor surface would reduce the system bit rate by a factor of about 10^{-3}, resulting in a bit count per frame of about $(1 \times 10^{+11})\ 10^{-3} = 10^{+8}$ electrons/frame.

We conclude that in order to measure surface contours to 10^{-3} inch accuracy, the sample attenuation must be no more than 10^{+4} higher than our model Lambertian surface. Sample attenuation in this system can be generated by surface gloss as well as by surface albedo. For example, a highly specular polished metal surface will return orders of magnitude less energy in the direction of the tracker than a Lambertian reflector in most angular orientations, even though the metal reflects most of the incident light.

The illuminator has 10 glass/air surfaces, 2 aluminum mirrors, and one chopper, netting a transmissive efficiency of $0.96^{10} \times 0.8^{2} \times 0.5^{1} = 0.21$; it focuses $5 \times 10^{-3} \times 0.21 = 1.1 \times 10^{-3}$ watts into a .001" diameter spot on the rotor surface with an area of 7.9×10^{-7} in ^{2}. Hence the energy density in the illuminated spot is $1.1 \times 10^{-3} / 7.9 \times 10^{-7} = 1400$ watts/in ^{2}. By way of comparison, noon sunlight at sea level on a clear day has an energy density of about 0.5 watts/in ^{2}.

Preliminary reflectance measurements on six rotor material samples indicated that all of them exhibited ample reflectance for electro-optical contouring. In order to demonstrate this finding, we made photometric measurements on all six samples at three different positions in two different orientations, as shown in Figure 14. The three positions were at the location of the leading edge, mid-section, and trailing edge of a rotor with a 48" chord. The two orientations were with an angle of 10° between the test surface and the axes of the illuminator and the tracker.

To put the measurements of Tracker output (Table 16) in context, we note that 0.1 is the smallest tracker output level at which the System can make contour measurements to an accuracy of 0.001" in 0.001 second.

TABLE 16
GONIOMETRIC REFLECTANCE OF SIX HELICOPTER ROTOR SURFACE MATERIALS

Tabulation Of Relative Tracker Voltage (six samples at three locations in two orientations).

Sample No.		1	2	3	4	5	6
Leading Edge	10°IL	140	350	120	140	220	15
	10°TR	4.8	19	22	25	30	1.8
Mid-Section	10°IL	61	780	220	190	300	17
	10°TR	4.4	140	40	56	76	7.0
Trailing Edge	10°IL	20	580	58	92	120	16
	10°TR	0.9	52	21	23	21	1.4

Sample No. 1 is "graphite" (black semigloss)
Sample No. 2 is "glass cloth & resin" (silvery translucent weave)
Sample No. 3 is "filament wound basket weave & resin" (white translucent)
Sample No. 4 is "undirectional glass & resin" (yellowish ivory translucent)
Sample No. 5 is "cloth prepreg" (yellowish translucent)
Sample No. 6 is Bell Rotor No. 654-015-001-1 (matte aluminum-32 finish)

Cylinder Contour Measurement

The results of the cylinder contour measurement are shown in Tables 17 and 18. The standard deviation of the error was .00014" for the first set of measurement data and .00020" for the second set of measurement data.

The repeatability of the system in measuring radial dimensions on this cylinder is 0.00010", as shown by the standard deviation of the differences between corresponding R values in Tables 17 and 18.

TABLE 17
CYLINDER CONTOUR DATA
RUN 1

POINT	IL	TR	BLC	XEOD	YEOD	R	E
1	57.5000	59.0825	39.9718	20.4075	31.6254	.50486	+.00006
2	57.4000	59.1336	39.9718	20.4656	31.5943	.50460	-.00020
3	57.3000	59.1965	39.9718	20.5283	31.5702	.50483	+.00003
4	57.2000	59.2733	39.9718	20.5965	31.5543	.50498	+.00013
5	57.1000	59.3668	39.9719	20.6711	31.5482	.50475	-.00005
6	57.0000	59.4805	39.9719	20.7536	31.5539	.50502	+.00022
7	56.9000	59.6273	39.9719	20.8491	31.5789	.50464	-.00016

σ = .00014"

Origin: X = 20.67602"
Y = 32.05293"

TABLE 18
CYLINDER CONTOUR DATA
RUN 2

POINT	IL	TR	BLC	XEOD	YEOD	R	E
1	57.5000	59.0827	39.9718	20.4076	31.6255	.50478	-.00002
2	57.4000	59.1336	39.9718	20.4656	31.5943	.50463	-.00017
3	57.3000	59.1967	39.9718	20.5284	31.5703	.50470	-.00010
4	57.2000	59.2730	39.9718	20.5963	31.5541	.50513	+.00033
5	57.1000	59.3667	39.9719	20.6711	31.5482	.50469	-.00011
6	57.0000	59.4804	39.9719	20.7536	31.5538	.50502	+.00022
7	56.9000	59.6271	39.9719	20.8490	31.5788	.50456	-.00024

σ = .00020"

Origin: X = 20.67624"
Y = 32.05286"

11. DISCUSSION OF RESULTS

The objective of Phase I of this program was to build and test an experimental model of a novel non-contacting, electro-optical measuring system which will contour helicopter rotor surfaces to an accuracy of ± .001".

Contour measurements made on actual rotor surfaces by the new system were compared with measurements made by a conventional contacting system; these measurements agreed to within the accuracy limits of the contacting system. Unfortunately, the contacting measuring system had known sources of error of the order of .004", and hence could not definitively check the absolute dimensional accuracy of the non-contacting system at that level. Furthermore, the rotor surfaces distorted under the localized pressure of the contacting probe; this contact distortion was particularly troublesome in the case of the Kaman Cobra Rotor Blade because of the flexibility of its black neoprene rubber leading edge.

An independent test of the non-contacting system's metrological integrity at the .001" level was made using repeated independent sets of contour measurements on the same rotor surface. These measurements exhibited repeatibility of about .0001" in the electro-optically measured contours. This demonstrated fact implies that any sources of error which may exist in the non-contacting system could be calibrated out if accurate standards could be found to check it against.

The new system was carefully studied during its design and testing in order to find and eliminate such sources of error.

A second independent test of the absolute accuracy of the non-contacting system was made on a precisely known non-rotor surface: a 1" diameter metal plug gauge. This test yielded electro-optical contour data which agreed with the known gauge's size and shape to about .0001".

Based on the above test data, it is concluded that the electro-optical system can indeed make surface contour measurements to an accuracy of ± .001".